

# Neutron Star Mergers as sites of $r$ -process Nucleosynthesis and Short Gamma-Ray Bursts

Kenta Hotokezaka<sup>1</sup>, Paz Beniamini<sup>2</sup>, and Tsvi Piran<sup>3</sup>

<sup>1</sup>Department of Astrophysical Sciences, Peyton Hall,  
Princeton University, Princeton, NJ 08544, USA

<sup>2</sup>Department of Physics, The George Washington University,  
Washington, DC 20052, USA

<sup>3</sup>Racah Institute of Physics, The Hebrew University of Jerusalem,  
Jerusalem 91904, Israel

January 8, 2018

## Abstract

Neutron star mergers have been long considered as promising sites of heavy  $r$ -process nucleosynthesis. We overview observational evidence supporting this scenario including: the total amount of  $r$ -process elements in the Galaxy, extreme metal poor stars, geological radioactive elemental abundances, dwarf galaxies, and short gamma-ray bursts (sGRBs). Recently, the advanced LIGO and Virgo observatories discovered a gravitational-wave signal of a neutron star merger, GW170817, as well as accompanying multi-wavelength electromagnetic (EM) counterparts. The ultra-violet, optical, and near infrared observations point to  $r$ -process elements that have been synthesized in the merger ejecta. The rate and ejected mass inferred from GW170817 and the EM counterparts are consistent with other observations. We find however that, within simple one zone chemical evolution models (based on merger rates with reasonable delay time distributions as expected from evolutionary models, or from observations of sGRBs), it is difficult to reconcile the current observations of the europium abundance history of Galactic stars for  $[\text{Fe}/\text{H}] \gtrsim -1$ . This implies that to account for the role of mergers in the Galactic chemical evolution, we need a Galactic model with multiple populations that have different spatial distributions and/or varying formation rates.

## 1 Introduction

Rapid neutron capture process (“ $r$ -process”) has been known as a basic formation process for the heaviest elements in the cosmos since the seminal work of B<sup>2</sup>FH (Burbidge et al., 1957) and Cameron (1957). The question in which astrophysical environment it actually occurs, however, has puzzled astrophysics ever since. For a long time core-collapse supernovae (cc-SNe) have been considered as the favored production site (Takahashi et al. 1994; Woosley et al. 1994; Hoffman et al. 1997; Freiburghaus et al. 1999a; Qian & Woosley 1996; Thompson et al. 2001; Fryer et al. 2006; Farouqi et al. 2010; Arcones & Martínez-Pinedo 2011; Wanajo 2013; Goriely & Janka 2016 and see also Qian & Wasserburg 2007; Arnould et al. 2007; Arcones & Thielemann 2013 for reviews). As an alternative site, Lattimer & Schramm (1974); Lattimer & Schramm (1976) suggested the decompression of cold neutron-rich matter ejected during the tidal disruption of a neutron star by a stellar mass black hole, a process that occurs in a similar way during the merger of two neutron stars (Symbalisty & Schramm 1982, see also Thielemann et al. 2017 for a recent review).

Eichler et al. (1989) placed compact binary mergers in a broader astrophysical context suggesting that Gamma-ray Bursts (GRBs), that at the time were believed to be of galactic origin, are extragalactic. Furthermore, they suggested that in addition to bursts of gravitational waves and neutrinos and the production of (heavy)  $r$ -process material these mergers are the engines of GRBs.

Today it is believed that indeed the subclass of short duration bursts (sGRBs) arise from mergers (Nakar, 2007; Berger, 2014).

Eichler et al. (1989) estimated the rate of mergers and suggested that these events could be major sources of  $r$ -process material. In the first detailed calculation of mass ejection from a merger, Rosswog et al. (1999) found that  $\sim 10^{-2}M_{\odot}$  become unbound during a merger event due to gravitational torques and hydrodynamic interaction (this is referred to as “dynamical ejecta” in the following). A follow-up work by Freiburghaus et al. (1999b) performed the first nuclear network calculations based on hydrodynamics simulations showing that the resulting abundance patterns agree well with the observed solar system abundances for  $A > 130$  and, folding the ejecta masses with the estimated merger rates, this indicated that, indeed, neutron star mergers could represent a major source of cosmic  $r$ -process elements.

At the same time, Li & Paczyński (1998) suggested that the radioactive decay of the neutron-rich nuclei in these “dynamical ejecta” would produce a macronova (also referred to as kilonova): a short lived optical - near infrared (nIR) weak supernova-like signal. The heating rate of radioactive decay of  $r$ -process elements was addressed by Metzger et al. (2010a). Studies of kilonova/macronova evolution revealed its prospects for detectability (Li & Paczyński 1998; Kulkarni 2005; Metzger et al. 2010a; Roberts et al. 2011; Goriely et al. 2011; Piran et al. 2013; Barnes & Kasen 2013; Tanaka & Hotokezaka 2013; Grossman et al. 2014, see also Tanaka 2016 and Metzger 2017 for reviews). The large opacities of lanthanides produced via  $r$ -process nucleosynthesis lead to the conclusion that the main emission will be in the nIR band peaking a week later than the merger (Kasen et al., 2013; Barnes & Kasen, 2013; Tanaka & Hotokezaka, 2013). Observation of such a nIR signal following a sGRB is by itself an indication that a significant amount of heavy  $r$ -process material was produced in this event.

On June 3rd 2013, the *Swift* satellite detected a relatively nearby sGRB (Melandri et al., 2013) at a redshift of 0.356. At 9 days after the burst ( $\approx 6.6$  days in the local rest frame), the *Hubble Space Telescope* detected a nIR point source with an apparent magnitude of  $H_{160,AB} = 25.73 \pm 0.2$  ( $M_{J,AB} \approx -15.35$ ; Tanvir et al. 2013; Berger et al. 2013), corresponding to an intrinsic luminosity of  $\approx 10^{41}$  erg/s. The upper limit on the  $r$ -band emission at the same time,  $R_{606,AB} > 28.5$ , suggests that the regular afterglow has decayed by this time. The nIR excess at 9 days after the burst was interpreted by both groups as tentative evidence for a Li-Paczynski kilonova/macronova (Tanvir et al., 2013; Berger et al., 2013).

Later on Yang et al. (2015) found an indication of a kilonova/macronova-like bump in the archival data of the afterglow of GRB 060614 and Jin et al. (2016) found another one in the afterglow of the sGRB 050709, the first sGRB from which an optical afterglow was observed (Fox et al., 2005). Jin et al. (2016) explored other sGRBs and concluded that kilonova/macronova candidates were observed in three out of three (or at most six) possible sGRBs that were sufficiently nearby and for which data were available. In addition, the sGRB 080503 was accompanied by an optical transient on a time scale of a few days (Perley et al., 2009). Although the redshift of this burst is unknown, the optical bump can be consistent with a macronova model assuming  $z = 0.25$  (Kasen et al., 2015). More recently, the nearby sGRB 160821B was found at  $z = 0.16$ . Kasliwal et al. (2017) reported a  $K_s$ -band detection at 4.3 days after the burst, which might arise from a kilonova/macronova. However, a detailed modeling of the afterglow using the multi-band data is necessary to interpret the origin of the emission.

During the past decade much effort has been invested in understanding the relevance and the implications of mergers to  $r$ -process (optical-nIR emissions; Li & Paczyński 1998; Metzger et al. 2010b; Roberts et al. 2011; Barnes & Kasen 2013; Grossman et al. 2014; Kasen et al. 2013; Piran et al. 2013; Tanaka & Hotokezaka 2013; Kasen et al. 2015; Barnes et al. 2016; Kawaguchi et al. 2016; Hotokezaka et al. 2017; Wollaeger et al. 2017; Tanaka et al. 2017, merger and mass ejection simulations; Rosswog et al. 2000; Shibata & Uryū 2000; Ruffert & Janka 2001; Rosswog 2005; Oechslin et al. 2007; Metzger et al. 2008; Dessart et al. 2009; Rezzolla et al. 2011; East & Pretorius 2012; Bauswein et al. 2013; Hotokezaka et al. 2013a; Rosswog et al. 2013; Rosswog 2013; Metzger & Fernández 2014; Fernández & Metzger 2013; ?; Foucart et al. 2014; Fernández et al. 2015; Just et al. 2015; Kawaguchi et al. 2015; Kiuchi et al. 2015; Kyutoku et al. 2015; Sekiguchi et al. 2015; Radice et al. 2016; Ruiz et al. 2016; Bovard et al. 2017; Ciolfi et al. 2017; Dietrich et al. 2017; Foucart et al. 2017; Fujibayashi et al. 2017; Kyutoku et al. 2017; Shibata et al. 2017; Siegel & Metzger 2017, and nucleosynthesis studies; Surman et al. 2008; Lee et al. 2009; Goriely et al. 2011; Korobkin et al.

2012; Caballero et al. 2012; Wanajo & Janka 2012; Malkus et al. 2012; Surman et al. 2013; Wanajo et al. 2014; Eichler et al. 2015; Lippuner & Roberts 2015; Wu et al. 2016; Lippuner et al. 2017). The picture that emerges from this wealth of studies is the following: a) the dynamical ejecta with their extreme neutron-richness provide excellent conditions for heavy ( $A \gtrsim 100$ )  $r$ -process and the resulting abundance pattern is largely independent of the specifics of the merging binary system (Goriely et al., 2011; Korobkin et al., 2012; Wanajo et al., 2014; Eichler et al., 2015; Bovard et al., 2017) and b) mergers provide additional nucleosynthesis channels such as neutrino-driven winds and the final dissolution of the accretion disk which is likely complement of the nucleosynthesis from the dynamical ejecta (Dessart et al., 2009; Fernández & Metzger, 2013; Perego et al., 2014; Fernández et al., 2015; Just et al., 2015; Wu et al., 2016; Lippuner et al., 2017; Fujibayashi et al., 2017; Shibata et al., 2017; Siegel & Metzger, 2017). While details of the resulting isotopic abundances vary somewhat among different models, the overall picture of an expected robust  $r$ -process pattern that agrees with the observed abundance peaks arises in most calculations.

On 17th of August in 2017, a gravitational-wave signal from a binary neutron star merger was detected by the LIGO/Virgo detectors. Two seconds later, a weak short-duration  $\gamma$ -ray burst was found in the gravitational-wave localization area by the *Fermi* and *INTEGRAL* satellites (Abbott et al., 2017a; Goldstein et al., 2017; Savchenko et al., 2017). Although this burst, GRB 170817A, is extremely weak compared to short GRBs (the isotropic equivalent  $\gamma$ -ray energy is even smaller than the weakest short GRB by more than two orders of magnitude), the observed spectra provide the first evidence that a relativistic jet is produced by the central remnant after merger (Gottlieb et al., 2017; Bromberg et al., 2017). An optical-nIR counterpart, AT2017gfo, was discovered at  $\sim 11$  hr after the merger (Coulter et al., 2017; Soares-Santos et al., 2017; Valenti et al., 2017; Arcavi et al., 2017; Tanvir et al., 2017; Lipunov et al., 2017). A number of follow-up observations were conducted and the photometric light curves including the ultra-violet bands and spectral evolution were taken (Andreoni et al., 2017; Arcavi et al., 2017; Chornock et al., 2017; Coulter et al., 2017; Cowperthwaite et al., 2017; Drout et al., 2017; Evans et al., 2017; Kasliwal et al., 2017; Kilpatrick et al., 2017; Lipunov et al., 2017; McCully et al., 2017; Nicholl et al., 2017; Pian et al., 2017; Shappee et al., 2017; Smartt et al., 2017; Tanvir et al., 2017; Troja et al., 2017; Utsumi et al., 2017; Valenti et al., 2017). The observed features are broadly consistent with a kilonova/macronova model, indicating that  $r$ -process elements with a mass of  $\sim 0.05M_{\odot}$  have been synthesized in this event. Although no specific elements are identified in the signal, this supports that  $r$ -process elements are synthesized in merger ejecta and mergers predominately produce the cosmic  $r$ -process elements. At later times, X-ray (Troja et al., 2017; Evans et al., 2017; Haggard et al., 2017; Margutti et al., 2017) and radio counterparts (Hallinan et al., 2017; Alexander et al., 2017; Mooley et al., 2017) were also found at the same location of the optical-nIR counterpart. These non-thermal emissions arise most likely from the forward shock between the ejected outflow and interstellar medium (ISM). It is likely that the outflow producing this emission has been energized by a choked jet that has formed a cocoon. The radio and X-ray emissions around 100 days require a mildly relativistic outflow and this is also evidence for the existence of a (mildly) relativistic outflow associated with the merger (Mooley et al., 2017; Ruan et al., 2017).

Despite the growing consistency among different theory/simulation results – in favor of mergers, against cc-SNe – some reservations against the neutron star merger scenario have remained, mainly due to the unsettled question whether or not they are consistent with the Galactic chemical evolution (Qian, 2000; Argast et al., 2004; Matteucci et al., 2014; Hirai et al., 2015; Shen et al., 2015; van de Voort et al., 2015; Ishimaru et al., 2015; Wehmeyer et al., 2015; Cescutti et al., 2015; Côté et al., 2016). The large scatter in Eu abundances at low metallicities compared to that of  $\alpha$ -elements is consistent with the picture (where  $\alpha$  denotes light nuclei like C, O, and Mg), in which  $r$ -process elements are produced by phenomena that is much less frequent than normal cc-SNe (Piran et al., 2014). The most likely scenario for explaining the high europium abundances of extremely metal poor stars, is that they were formed in small dwarf galaxies that have merged with the Milky Way (van de Voort et al., 2015; Ishimaru et al., 2015; Shen et al., 2015; Naiman et al., 2017; Beniamini et al., 2017). In addition, the chemical abundance studies of dwarf galaxies (Tsujimoto & Shige-yama, 2014; Ji et al., 2016a; Roederer et al., 2016; Beniamini et al., 2016b, 2017; Hirai et al., 2017) and the abundance measurements of radioactive nuclides of the solar system materials (Paul et al., 2001; Turner et al., 2004, 2007; Brennecka et al., 2010; Wallner et al., 2015; Hotokezaka et al., 2015; Tissot et al., 2016; Tsujimoto et al., 2017) indicate that rare phenomena as the heavy  $r$ -process production

site. More recent works focus on the late chemical evolution in the Milky Way. The ratio of  $r$ -process elements to Fe,  $[\text{Eu}/\text{Fe}]$ , declines for  $[\text{Fe}/\text{H}] > -1$ , where  $[X/Y] = \log_{10}(N_X/N_Y) - \log_{10}(N_X/N_Y)_\odot$ ,  $N_X$  is the abundance of an element X, and  $\odot$  refers to the solar value. It has been questioned whether such a behavior is consistent with the expected merger history in the Milky Way (Côté et al., 2016; Komiya & Shigeeyama, 2016).

Our goal in this article is twofold. First we summarize the cumulative evidences supporting that  $r$ -process nucleosynthesis takes place in rare events in which a significant amount of  $r$ -process elements are produced in each event. Using the rate and mass ejection per event inferred from these measurements, we test the neutron star merger scenario for the origin of  $r$ -process elements in the cosmos. This evidence clearly rules out the normal cc-SNe scenario. Moreover, the rate agrees with merger estimates from galactic binary neutron stars, from sGRBs, and from GW170817. At the same time the amount of matter is consistent with the kilonova/macronova, AT2017gfo, and the candidates associated with cosmological sGRBs. Second, we turn to the Galactic chemical evolution of  $r$ -process elements at later times  $[\text{Fe}/\text{H}] \gtrsim -1$  and discuss whether the neutron star merger scenario can consistently explain the observed distribution of  $[\text{Eu}/\text{Fe}]$ .

## 2 $r$ -process production rate, sGRBs, and GW170817

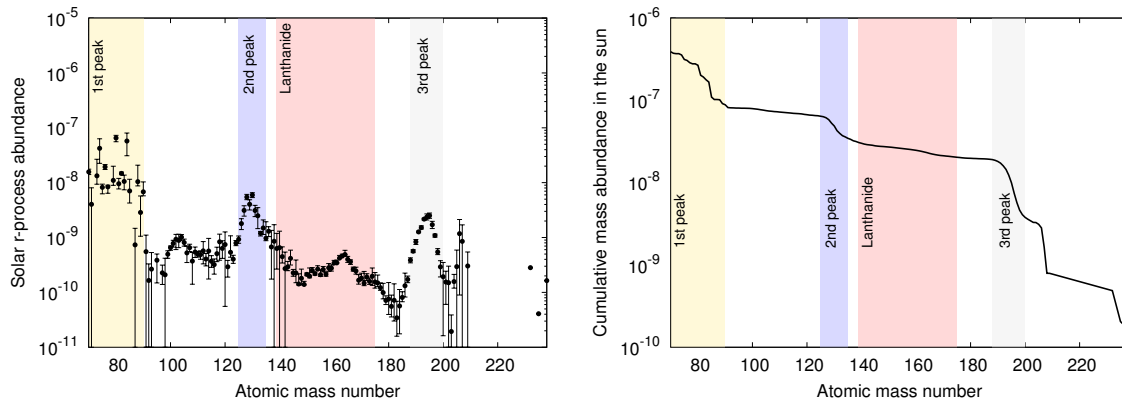


Figure 1: The solar abundance pattern of  $r$ -process elements (*left*) and its cumulative abundance (*right*). The solar  $r$ -process abundance pattern is taken from Goriely (1999); Lodders (2003).

Before discussing details, we describe here the  $r$ -process abundance pattern. Figure 1 shows the solar abundance pattern of  $r$ -process elements taken from (Goriely, 1999; Lodders, 2003). There are three peaks. For the solar abundance pattern, most of the mass of  $r$ -process elements ( $\sim 80\%$ ) is around the first peak. However, the abundance ratio of the first peak to the second peak of extreme metal poor stars, of which the abundance pattern likely reflects a single nucleosynthesis event, is often different from that of the solar pattern. Some of these stars exhibit abundance patterns beyond the second peak (heavy  $r$ -process) that are similar to the solar pattern. However, they don't contain similar amounts of the first peak elements as compared with expectations from the solar abundance pattern (e.g. Sneden et al. 2008 and references therein). At the same time, there are stars that contain a substantial amount of the first peak elements but do not show a significant enrichment of heavy  $r$ -process elements (e.g. Honda et al. 2006). This suggests that the ratio between “light” and “heavy”  $r$ -process abundances varies among events or there may be different kinds of astrophysical phenomena producing “light” and “heavy”  $r$ -process elements. For instance, electron capture and cc-SNe could produce a sufficient amount of “light”  $r$ -process elements (e.g. Roberts et al. 2010; Wanajo et al. 2011). Therefore, it is important to keep in mind that it is unclear what the minimal atomic mass number of elements produced by  $r$ -process events is.

Since rate estimates of  $r$ -process events are sensitive to the minimal atomic mass number assumed, we consider here two scenarios in which an astrophysical phenomenon predominantly produces (i) all the  $r$ -process elements ( $A_{\min} = 69$ ) and (ii) only heavy  $r$ -process elements ( $A_{\min} = 90$ ). The mass fractions of the lanthanides out of the total  $r$ -process elements for these two cases are

$\approx 0.025$  and  $0.1$ , respectively. In the following, we test the neutron star merger scenario for the origin of (heavy)  $r$ -process elements. It is worth noting that numerical simulations of merger ejecta show that heavy  $r$ -process elements are robustly synthesized (Goriely et al., 2011; Korobkin et al., 2012; Perego et al., 2014; Wanajo et al., 2014; Eichler et al., 2015; Just et al., 2015; Wu et al., 2016; Siegel & Metzger, 2017). The first peak elements are not necessarily synthesized and their abundances depend on the ejection mechanism and on the nature of the remnant of mergers (e.g. Wanajo et al. 2014; Lippuner & Roberts 2015; Wu et al. 2016; Lippuner et al. 2017) so that mergers with different masses may produce different abundance patterns. Note that there are metal poor stars in which the abundance ratio of Th to Eu is larger than that of the sun, the so-called “actinide boost stars” (e.g. Hill et al. 2002; Roederer et al. 2009). The variation in elemental abundances beyond the third  $r$ -process peak elements does not affect the mass estimates but they suggest that there are  $r$ -process events that produce larger amounts of very heavy elements.

## 2.1 Production rate inferred from $r$ -process measurements

Astrophysical observations and geological measurements provide evidence that  $r$ -process elements are produced in rare events in each one of those a significant amount of  $r$ -process elements (a few percent of solar masses) are produced. These observations support the merger scenario. In this section, we briefly summarize the observations and demonstrate their compatibility with each other and with the merger scenario. The results are summarized in Figs. 2 and 3.

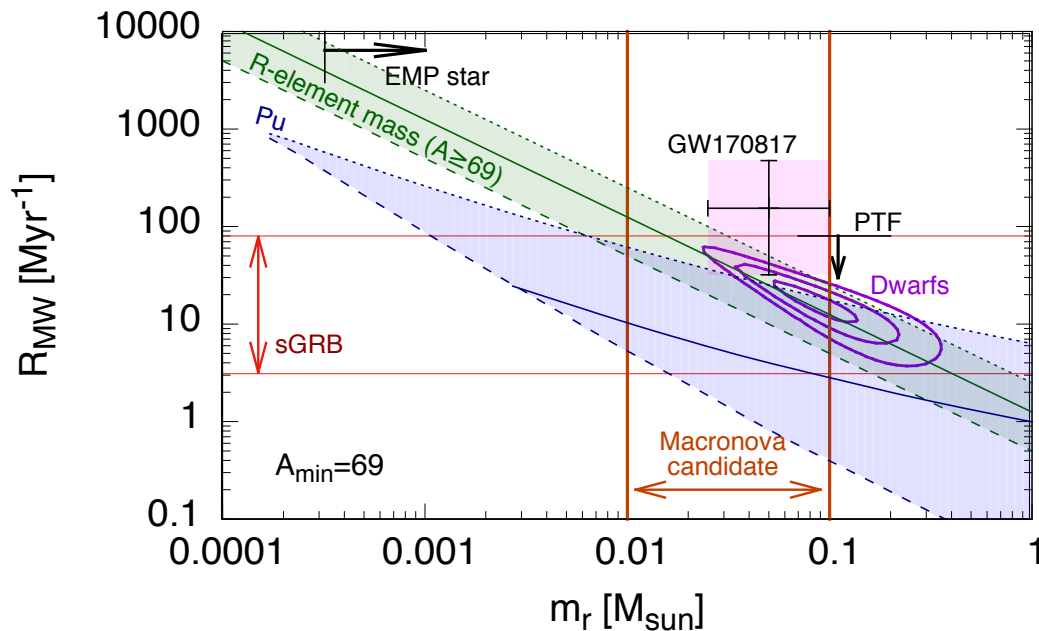


Figure 2: The rate of  $r$ -process production events in the Milky Way and the mass produced per event inferred from various measurements (see the text for details and also Hotokezaka et al. 2015). Here, we assume  $r$ -process elements with the solar abundance pattern for  $A \geq 69$  (including the first peak  $r$ -process elements) are produced in each event. For GW170817, we take the rate estimated with the 90% confidence interval (Abbott et al., 2017b) and the mass estimate of  $\approx 0.05M_{\odot}$  with an uncertainty of a factor of 2. To convert the volumetric event rate  $\text{Gpc}^{-3}\text{yr}^{-1}$  to the galactic event rate, we use the number density of Milky-Way like galaxies of  $\approx 0.01\text{Mpc}^{-3}$ .

(i) *The total mass of  $r$ -process elements in the Milky Way:* The total mass of  $r$ -process elements in the Milky Way gives a rough estimate for the product of the event rate  $R_{\text{MW}}$  and the average mass produced by each event  $m_r$ :  $M_{\text{tot},r} \sim t_{\text{MW}} \cdot R_{\text{MW}} \cdot m_r$ , where  $t_{\text{MW}} \approx 10\text{Gyr}$  is the age of the Milky Way (e.g. Eichler et al. 1989; Bauswein et al. 2014; Hotokezaka et al. 2015; Rosswog

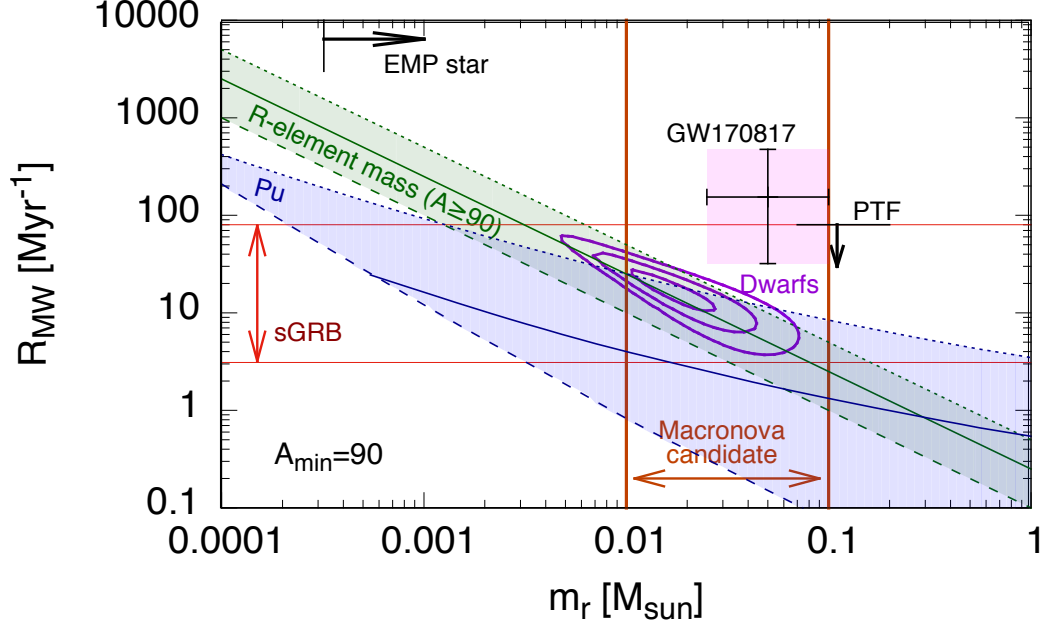


Figure 3: Same as Figure 2 but for the case that only heavy  $r$ -process elements  $A \geq 90$  (excluding the first peak  $r$ -process elements) are produced in each event.

et al. 2017a). This approximate relation assumes that the mass loss due to the galactic wind is negligible compared to the total stellar mass of the Galactic disk, where we take the total mass of  $\approx 6 \cdot 10^{10} M_{\odot}$  (McMillan, 2011). Assuming that the mean  $r$ -process abundance of stars in the Galactic disk is the solar value (e.g. Venn et al. 2004; Battistini & Bensby 2016 for europium abundances of local stars), the total mass is estimated as  $\sim 23000 (5000) M_{\odot}$  for elements with  $A \geq 69 (90)$ . This corresponds to

$$\begin{aligned} R_{\text{MW}} &\sim 230 \text{ Myr}^{-1} (m_r / 0.01 M_{\odot})^{-1} \quad (A_{\text{min}} \geq 69), \\ R_{\text{MW}} &\sim 50 \text{ Myr}^{-1} (m_r / 0.01 M_{\odot})^{-1} \quad (A_{\text{min}} \geq 90). \end{aligned} \quad (1)$$

The estimate involves an uncertainty in the mean abundance of  $r$ -process elements of the Milky Way stars due to the limited sample. Note that this rate is averaged over the Milky Way lifetime so that the present-day Galactic  $r$ -process event rate does not necessarily match this rate and the relation depends on the redshift distribution of  $r$ -process production events. For the neutron star merger scenario, it is important to note that some neutron star mergers do not contribute to the  $r$ -process enrichment of the ISM because they escape from the Galactic disk due to the natal kicks (see §3). This effect may result in an underestimate of  $R_{\text{MW}}$ .

(ii) *Galactic extremely metal-poor stars*: The large dispersion in the [Eu/Fe] abundances of extremely metal poor stars compared to that of  $[\alpha/\text{Fe}]$  suggests that  $r$ -process production events are rarer than cc-SNe in which  $\alpha$ -elements are produced (e.g. Sneden et al. 2008; Piran et al. 2014). The rate estimate using this distribution depends strongly on the mixing time scale of the ISM and the history of the Milky Way at early times. Macias & Ramirez-Ruiz (2016) obtained a lower limit on the mass of  $r$ -process elements produced per event of  $\sim 0.3 \cdot 10^{-3} M_{\odot}$  using the largest value of [Eu/H] obtained from low metallicity stars. This estimate is valid as long as  $r$ -process elements are produced in explosions with kinetic energy of  $\gtrsim 10^{50}$  erg within the metal poor environment. Comparing this lower limit with Eq. (1) yields  $R_{\text{MW}} < 1500 \text{ Myr}^{-1}$ , far smaller than the galactic cc-SN rate,  $\sim 2.8 \cdot 10^4 \text{ Myr}^{-1}$  (Li et al., 2011), but consistent with mergers.

Previous studies have suggested that metal poor stars in the Galactic halo originate from tidally disrupted dwarf galaxies that merged with the Milky Way (Frebel et al., 2010a; van de Voort et al., 2015; Ishimaru et al., 2015; Hirai et al., 2017). The low event rate of  $r$ -process events (compared with

SNe) implies that only a small fraction of those dwarfs would have a single  $r$ -process event in their history. However, in those that do, the  $r$ -process enrichment could become extremely large. Indeed, assuming that this is the origin of Galactic halo metal poor stars, Beniamini et al. (2017) have shown that the resulting abundance is consistent with both the mean value and the fluctuations of  $[\text{Eu}/\text{Fe}]$  in halo metal poor stars, supporting the hypothesis that UFDs are the dominant “building blocks” of the Galactic halo.

(iii) *Radioactive elements in the early solar system and in deep sea floor:* The abundance of radioactive elements in the ISM at a given location is determined by their local production history on the time scale of their mean lives rather than the whole production history. Therefore, the abundance measurements of radioactive elements allow us to break the degeneracy between  $R_{\text{MW}}$  and  $m_r$  that appears in Eq. (1). There are two kinds of measurements of radioactive  $r$ -process elements. Their abundances during the formation of the solar system can be inferred from those of the daughter nuclides in the early solar system material, e.g., meteorites and ancient rocks (Turner et al., 2004, 2007; Brennecka et al., 2010; Tissot et al., 2016). The abundance measurements of  $^{129}\text{I}$  ( $t_{1/2} = 15.7$  Myr),  $^{232}\text{Th}$  (14 Gyr),  $^{235}\text{U}$  (704 Myr),  $^{238}\text{U}$  (4.5 Gyr),  $^{244}\text{Pu}$  (81 Myr), and  $^{247}\text{Cm}$  (15.6 Myr) can constrain the rate of  $r$ -process production events in the vicinity of the early solar system (e.g. Cowan et al. 1991; Wasserburg et al. 1996). In particular, a relatively large abundance ratio of  $^{244}\text{Pu}$  to  $^{238}\text{U}$  of 0.008 implies that the time delay between the  $r$ -process production and the formation of the early solar material is not much longer than 81 Myr. On the other hand, a tiny amount of  $^{129}\text{I}$  and  $^{247}\text{Cm}$  implies that the time delay is much longer than 20 Myr (Tissot et al., 2016). A time delay  $\tau_{\text{delay}} \sim 100$  Myr consistently explains these abundance measurements. This time delay can be approximately translated to the production rate in the Milky Way,  $R_{\text{MW}}$  (Hotokezaka et al., 2015):

$$\tau_{\text{delay}} \approx 120 \text{ Myr} (R_{\text{MW}}/100 \text{ Myr}^{-1})^{-2/5} (\alpha_t/0.1)^{-3/5} (v_t/7 \text{ km/s})^{-3/5} (H/0.2 \text{ kpc})^{-3/5}, \quad (2)$$

where  $v_t$  is the typical turbulent velocity of the ISM,  $H$  is the scale height of the ISM disk, and  $\alpha_t$  is the mixing length parameter.

Live radioactive elements, e.g.,  $^{60}\text{Fe}$  and  $^{244}\text{Pu}$ , are currently accreted by the solar system and accumulate in the Earth’s deep sea floor (see Ellis et al. 1996 for an earlier study and Fitoussi et al. 2008; Fry et al. 2016; Wallner et al. 2016; Schulreich et al. 2017 for studies on  $^{60}\text{Fe}$ ). While  $^{60}\text{Fe}$  is relatively short lived and is likely produced by SNe,  $^{244}\text{Pu}$  is perfectly suited for our purpose. Measurements of the current deposition rate averaged over the last 25 Myr show that the abundance of  $^{244}\text{Pu}$  in the ISM that accretes now on the solar system is much lower ( $\sim 10^{-2}$ ) than the abundance at the time of the formation of the solar system (Paul et al., 2001; Wallner et al., 2015). Such a large fluctuation in  $^{244}\text{Pu}$  abundances is consistent with a low event rate of  $r$ -process production. Hotokezaka et al. (2015) found the range of values of  $R_{\text{MW}}$  and  $m_r$  that are consistent with both early solar system and current observations (see also Tsujimoto et al. 2017). These values are shown in Figs. 2 and 3.

We should note that there are unknown factors in this calculation: (i) the ISM mixing parameter, (ii) the penetration efficiency of dust grains containing  $^{244}\text{Pu}$  from the ISM to the Earth’s orbit, (iii) the local ISM density where the solar system has been traveling during the last 25 Myr, and (iv) the star formation history in the solar neighborhood. The effect of these factors on the rate and ejecta mass estimate is shown in Hotokezaka et al. (2015).

(iv)  *$r$ -process abundances of dwarf galaxies:* The abundance of  $r$ -process elements of dwarf satellite galaxies of the Milky Way provides another estimate. The mean value of  $[\text{Eu}/\text{H}]$  of the observed stars of classical dwarf galaxies is between  $-1.5$  to  $-0.5$  (Shetrone et al., 2001, 2003; Venn et al., 2004; Letarte et al., 2010; Tsujimoto et al., 2015). Among ultra-faint dwarf (UFD) galaxies, Ji et al. (2016a) discovered  $r$ -process enrichment in Reticulum 2 with a mean of  $[\text{Eu}/\text{H}]$  of  $\sim -1$  (see also Ji et al. 2016b; Roederer et al. 2016). An  $r$ -process enriched star was recently found in another UFD, Tucana III (Hansen et al., 2017). However, only upper limits of  $\lesssim -2$  have been obtained for other ultra-faint dwarfs (Frebel et al., 2010b, 2014; Roederer & Kirby, 2014). As these ultra-faint dwarfs contain several hundreds to ten thousands stars, these observations suggest that the  $r$ -process production rate is rarer than one event per  $10^4$  stars formed (see Fig. 4). Using a maximum likelihood analysis, Beniamini et al. (2016b) estimated  $R_{\text{MW}}$  and  $m_r$  that are consistent

with the  $r$ -process elements distribution of dwarf galaxies. They find that the rate is  $\approx 1$  per  $10^3$  cc-SNe, corresponding to  $R_{\text{MW}} \approx 20 \text{ Myr}^{-1}$  (using a Galactic cc-SNe rate of  $\approx 2.8$  SNe per century (Li et al., 2011)).

The intersection of this range with the range given by Eq. (1) is at the same range of values given by the  $^{244}\text{Pu}$  estimate. Figures 2 and 3 demonstrate a remarkable consistency between different and independent estimates of the rate of  $r$ -process nucleosynthesis events and the amount of matter produced in each event. The values show clearly that regular cc-SNe can be ruled out as the sites of (heavy)  $r$ -process nucleosynthesis.

Note that Beniamini et al. (2016b) assumed that the  $r$ -process elements produced are fully mixed with the ISM of which the total mass is proportional to the dark-matter halo mass within the half-light radius of the galaxy. However, it is still unclear whether this assumption is valid. If the mixing is less efficient, the estimated ejecta mass is smaller. On the other hand, the estimated ejecta mass is larger, if a significant fraction of the ejecta is lost from the galaxy. This issue has been addressed in a one zone analytical model (Beniamini et al., 2017), which suggests that these considerations do not strongly affect the rate and ejecta mass estimates (by a factor of  $\lesssim 2$ ). Numerical studies of the evolution of UFDs (e.g. Greif et al. 2010; Hirai et al. 2015; Safarzadeh & Scannapieco 2017) would be able to consider these issues in further detail. For the neutron merger scenario, other caveats in this estimate are (i) it is easier for neutron star binaries to escape from smaller dwarfs and (ii) to take place in UFD, mergers must occur within relatively short time scales  $\lesssim 1$  Gyr as UFDs have quenched their star formation  $\approx 10$  Gyr ago. These effects may result in an underestimate of the merger rate by a factor of a few to  $\sim 20$  (e.g. Beniamini et al. 2016a and see §3).

While the measurements described above indicate that (heavy)  $r$ -process elements are produced in rare events and support the neutron star merger scenario, this does not rule out rare types of core collapse events as the source of  $r$ -process, e.g., strongly magnetized neutron star formation and black hole formation (Suzuki & Nagataki, 2005; Wanajo & Janka, 2012; Winteler et al., 2012; Vlasov et al., 2014; Nishimura et al., 2015; Fujibayashi et al., 2015; Mösta et al., 2017; Vlasov et al., 2017). However, apart from speculating about this possibility, it is not clear what is the expected rate and the amount of  $r$ -process elements produced in those phenomena.

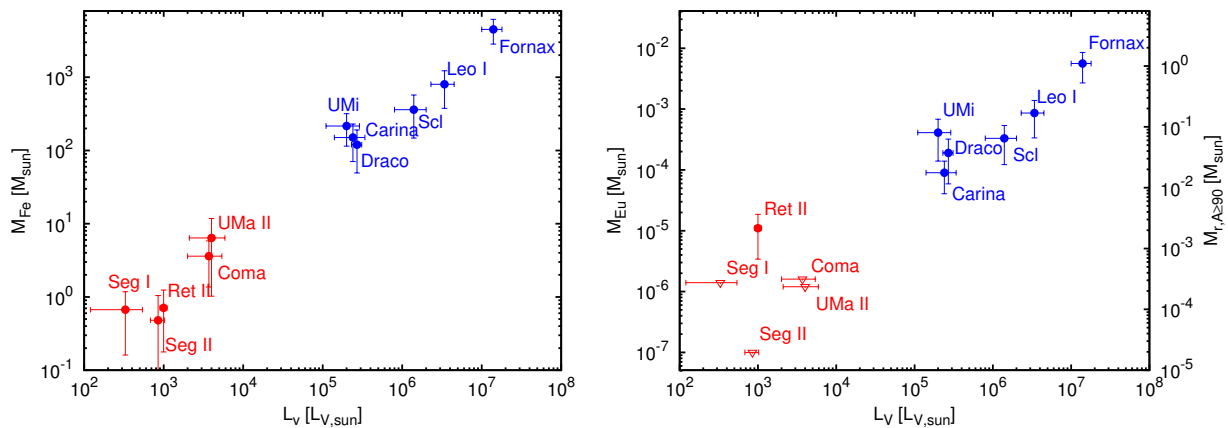


Figure 4: Iron (*left*) and europium (*right*) masses produced in dwarf galaxies. The horizontal axis shows the total V-band luminosity of each galaxy. Blue and red points depict the classical dwarfs and UFDs respectively. Open triangles show upper limits on the masses. The figures are taken from Beniamini et al. (2016b).

## 2.2 Short GRB rate and kilonova/macronova candidates

Neutron star mergers are considered as the classical progenitors of sGRBs (Eichler et al., 1989). Information on their rate and possible mass ejection that takes place in them can shed additional light on the problem at hand.

(i) *Rate:* Observed short GRBs occur typically at a redshift of  $\approx 0.5$ , which is much further than GW170817. Wanderman & Piran (2015) find  $R_{\text{sGRB}} = 6 \pm 2 \text{ Gpc}^{-3} \text{ yr}^{-1}$  which agrees within a factor of 2 with various previous estimates (Guetta & Piran, 2006; Nakar et al., 2006; Guetta & Stella, 2009). Assuming an unknown beaming correction  $f_b = (1 - \cos \theta_j)$  to be 100 (e.g. Fong et al. 2014), the rate is  $600 \text{ Gpc}^{-3} \text{ yr}^{-1} (f_b^{-1}/100)$  and the Galactic rate is  $\approx 60 \text{ Myr}^{-1} (f_b^{-1}/100)$ , using the density of galaxies of  $0.01 \text{ Mpc}^{-3}$ . This estimate depends on the luminosity function of sGRBs and particularly on the lowest peak luminosity of sGRBs. Wanderman & Piran (2015) adopt  $5 \cdot 10^{49} \text{ erg/s}$ , with which the *Swift* sGRB rate does not exceed the BATSE rate. Note that the luminosity of the  $\gamma$ -ray pulse associated with GW170817 is much lower than this value. However, the lack of the X-ray afterglow until 9 days after the merger suggests (if there was one) did not point towards Earth (Troja et al., 2017; Evans et al., 2017; Haggard et al., 2017; Margutti et al., 2017). Therefore, we should keep in mind that this  $\gamma$ -ray burst, GRB 170817A, is not the typical sGRB but a new type of GRBs, a *low-luminosity* short GRB.

(ii) *Time delay:* The population of sGRB hosts shows evidence for a time delay between the burst and the progenitor formation. The most notable one is that a fraction of bursts ( $\sim 20\%$ ) take place in early-type galaxies, where star formation is no longer active (e.g. Berger 2014). A comparison of the redshift distribution of sGRBs to the cosmic star formation history, Wanderman & Piran (2015) and Ghirlanda et al. (2016) show that there is a time delay between the two. A delay-time distribution  $\propto t^{-1}$  with a minimal time delay of 20 Myr is consistent with the observed rate. However, these parameters, the slope of the time delay distribution and the minimal delay time are rather weakly constrained (Wanderman & Piran, 2015).

(iii) *Ejecta mass estimate:* Observations of optical-nIR signatures that follow sGRBs and can be considered as kilonova/macronova candidates, GRB 080503 (Perley et al. 2009; but its redshift is unknown), GRB130603B (Tanvir et al., 2013; Berger et al., 2013), GRB 060614 (Gal-Yam et al., 2006; Yang et al., 2015; Jin et al., 2015), GRB 050709 (Fox et al., 2005; Watson et al., 2006; Jin et al., 2016), and GRB160821B (Kasliwal et al., 2017), provide estimates of the amount of matter ejected in mergers,  $m_r$ , from the observed light curves. The estimated values are  $0.01 \lesssim m_r \lesssim 0.1 M_\odot$  (Tanvir et al., 2013; Berger et al., 2013; Hotokezaka et al., 2013b; Kasen et al., 2015; Yang et al., 2015; Jin et al., 2016; Kasliwal et al., 2017). These values are shown in Fig. 2. Therefore, if the kilonova/macronova interpretation is correct (all current kilonovae/macronovae identifications, apart from AT2017gfo, are based on just a single or at most a few data points), then when combined with the rate estimates, mergers are the dominant source of heavy  $r$ -process material in the universe. Note that the optical-nIR bumps of GRB 050709, 130603B, and 170821B are roughly consistent with the photometric light curve of AT2017gfo. The optical bump of GRB 060614 is much brighter than AT2017gfo. Such a bright signal requires a larger ejecta mass and may be associated with a black hole-neutron star merger (Yang et al., 2015; Jin et al., 2015).

The radio counterparts to kilonovae/macronovae are expected to arise on time scales from weeks to years (Nakar & Piran, 2011). The follow-up radio observations for sGRBs have not detected late-time radio flares (Metzger & Bower, 2013; Horesh et al., 2016; Fong et al., 2016). These upper limits constrain the kinetic energy of the merger outflows  $\lesssim 10^{52} - 10^{53} \text{ erg}$ , which is much larger than the ones expected for dynamical ejecta but rules out the existence of a magnetar central engine.

(iv) *Evidence for mass surrounding sGRBs:* Moharana and Piran (2017)(Moharana & Piran, 2017) have recently shown that the duration distribution of sGRBs shows a plateau at short durations (less than 0.4 s). This can be interpreted as the effect of a jet penetration through an engulfing envelope of surrounding matter. Scaling from corresponding estimates for LGRBs (Bromberg et al., 2011) they find  $t_{\text{break}} = 0.4(L/10^{49} \text{ erg})^{-1/3}(\theta/10^\circ)^{4/3}(R/10^9 \text{ cm})^{2/3}(m_r/0.1 M_\odot)^{1/3} \text{ s}$ , where  $L$  and  $\theta$  are the energy and opening angle of the jet and  $m_r$  and  $R$  are mass and size of the surrounding material. This results suggests the existence of ejecta with  $\sim 0.1 M_\odot$  surrounding the merger.

### 2.3 GW170817 and its electromagnetic counterparts

On 17th of August in 2017, a gravitational-wave signal from a binary neutron star merger was detected by the advanced LIGO/Virgo detectors (Abbott et al., 2017b). The total mass and mass ratio of the binary are determined as  $2.74^{+0.04}_{-0.01} M_\odot$  ( $2.82^{+0.47}_{-0.09} M_\odot$ ) and  $0.7 - 1.0$  ( $0.4 - 1.0$ ) for the  $|\chi| \leq 0.05$  (0.89) prior (Abbott et al., 2017b). The total mass is similar to those measured in Galactic binary neutron stars (e.g. Özel et al. 2012; Tauris et al. 2017). The gravitational-wave

luminosity distance to the source is  $40_{-14}^{+8}$  Mpc. About two seconds later, a weak short-duration  $\gamma$ -ray pulse, GRB 170817A, was found by the *Fermi* GBM (Abbott et al., 2017a; Goldstein et al., 2017). A  $\gamma$ -ray signal was also found in the data of the *INTEGRAL* satellite (Savchenko et al., 2017). The localization area of GRB 170817A is consistent with the area determined by LIGO and Virgo. Although GRB 170817A is extremely weak compared to sGRBs (the isotropic equivalent  $\gamma$ -ray energy is smaller than the weakest sGRB by more than two orders of magnitude), the observed  $\gamma$ -rays indicated that a relativistic outflow was produced (Kasliwal et al., 2017; Gottlieb et al., 2017). An optical-nIR counterpart (AT2017gfo) was discovered at  $\sim 11$  hr after the merger (Coulter et al., 2017; Soares-Santos et al., 2017; Valenti et al., 2017; Arcavi et al., 2017; Tanvir et al., 2017; Lipunov et al., 2017). This enabled the identification of the host galaxy NGC 4993, which is located at a distance consistent with  $40_{-14}^{+8}$  Mpc (Hjorth et al., 2017). Numerous follow-up observations were conducted and the photometric light curves (Andreoni et al., 2017; Arcavi et al., 2017; Cowperthwaite et al., 2017; Evans et al., 2017; Lipunov et al., 2017; Kasliwal et al., 2017; Kilpatrick et al., 2017; Smartt et al., 2017; Valenti et al., 2017; Drout et al., 2017; Pian et al., 2017; Coulter et al., 2017; Tanvir et al., 2017; Utsumi et al., 2017) and spectral evolution (Andreoni et al., 2017; Buckley et al., 2017; Chornock et al., 2017; Kilpatrick et al., 2017; Nicholl et al., 2017; Shappee et al., 2017; Smartt et al., 2017; Kasliwal et al., 2017; McCully et al., 2017; Pian et al., 2017; Tanvir et al., 2017; Troja et al., 2017; Valenti et al., 2017; Abbott et al., 2017) are broadly consistent with a kilonova/macronova model (see, e.g., Kasen et al. 2017; Tanaka et al. 2017 for modelings). At later times, an X-ray counterpart was discovered by the *Chandra X-ray Observatory* (Troja et al., 2017) and a radio counterpart was discovered by the Karl G. Jansky Very Large Array (Hallinan et al., 2017) at the same location of AT2017gfo (see also Evans et al. 2017; Haggard et al. 2017; Margutti et al. 2017; Ruan et al. 2017 for the X-ray observations and Alexander et al. 2017; Kim et al. 2017; Mooley et al. 2017 for the radio observations). These emissions are most likely arising from the forward shock between the ejected outflow and ISM (see, e.g., Kasliwal et al. 2017 for an interpretation of the multi-wavelength observations).

(i) *Rate and time delay:* The rate of binary neutron star mergers as implied from GW170817 is estimated as  $1540_{-1220}^{+3200}$  Gpc $^{-3}$  yr $^{-1}$ . This can be compared with estimates from the observed population of binary pulsars (Narayan et al., 1991; Phinney, 1991). Recent estimates (Abadie et al., 2010) suggest  $\approx 1 - 10^3$  Myr $^{-1}$ , which is broadly consistent with GW170817 (see also Kim et al. 2015). Given this rate and the estimate of the ejected  $r$ -process mass for AT2017gfo (see below), neutron star mergers could predominantly produce  $r$ -process elements in the Milky Way (Figs. 2 and 3 and see also Côté et al. 2017; Rosswog et al. 2017b). It is worth noting that the bright optical signal of AT2017gfo and the estimated rate suggest that optical transients similar to AT2017gfo could have been observed by optical transient surveys. However, Kasliwal *et al.* (2017) (Kasliwal et al., 2017) did not find such objects in the database of the Palomar Transient Factory, indicating that the rate is  $\lesssim 800$  Gpc $^{-3}$  yr $^{-1}$ .

The host galaxy properties have an implication on the time delay between the merger and progenitor formation. NGC 4993 is an S0-type galaxy and its current star formation rate, averaged over the last 100 Myr, is quite low  $\sim 0.01 M_{\odot}$  yr $^{-1}$  (Blanchard et al., 2017). Levan et al. (2017) have shown that the galaxy is dominated by an old stellar population and a very small fraction of stars ( $\ll 1\%$  of the stellar mass) were formed recently  $\lesssim 500$  Myr (see also Blanchard et al. 2017 and Pan et al. 2017). In addition, there is no young stellar mass system around the location of AT2017gfo (Levan et al., 2017). Therefore, GW170817 is likely to have a merger time of  $\sim 1-10$  Gyr (Blanchard et al., 2017; Levan et al., 2017; Pan et al., 2017). Finally, the projected distance of the merger of 2 kpc away from the center of the host galaxy indicates that the system did not receive a strong natal kick of  $\gtrsim 200$  km/s (Blanchard et al., 2017; Levan et al., 2017; Pan et al., 2017; Abbott et al., 2017).

(ii) *Ejecta mass and composition:* The kilonova/macronova light curves approximately satisfy the following relations for a given ejecta mass, velocity, and opacity. The light curve rises on a diffusion timescale:

$$t_p \approx \sqrt{\frac{\xi \kappa M_{\text{ej}}}{4\pi c v_{\text{ej}}}} \approx 5 \text{ days } \xi^{1/2} \left( \frac{\kappa}{10 \text{ cm}^2/\text{g}} \right)^{1/2} \left( \frac{M_{\text{ej}}}{0.01 M_{\odot}} \right)^{1/2} \left( \frac{v_{\text{ej}}}{0.1c} \right)^{-1/2}, \quad (3)$$

where  $\kappa$  and  $v_{\text{ej}}$  are the ejecta's opacity and velocity, and  $\xi$  is an order unity parameter depending

on the ejecta’s density profile. The luminosity and the effective temperature are given as

$$L_{\text{bol}}(t > t_p) \approx M_{\text{ej}} \cdot \dot{Q}(t) \approx 2.5 \cdot 10^{40} \text{ erg/s} \left( \frac{t_p}{5 \text{ day}} \right)^{-1.3} \left( \frac{M_{\text{ej}}}{0.01 M_{\odot}} \right), \quad (4)$$

$$T_{\text{eff}}(t_p) \approx \left( \frac{L_{\text{bol}}(t_p)}{4\pi\sigma v_{\text{ej}}^2 t_p^2} \right)^{1/4} \approx 2200 \text{ K} \left( \frac{L_{\text{bol,p}}}{2.5 \cdot 10^{40} \text{ erg/s}} \right)^{1/4} \left( \frac{v_{\text{ej}}}{0.1c} \right)^{-1/2} \left( \frac{t_p}{5 \text{ day}} \right)^{-1/2}, \quad (5)$$

where the  $\dot{Q}$  is the radioactive heating rate per unit mass and  $\sigma$  is the Stefan-Boltzmann constant. Here, we use  $\dot{Q}(t) \approx 10^{10} t_{\text{day}}^{-1.3} \text{ erg/s/g}$ , which is a general feature of  $\beta$  decay heating rate resulted from a statistical ensemble of many  $r$ -process decay chains (e.g. Metzger et al. 2010b; Korobkin et al. 2012; Hotokezaka et al. 2017). Note that the specific heating rate depends on the thermalization efficiency, which varies with time because of the  $\gamma$ -ray escape, the inefficiency of the electrons’ thermalization, and the contribution of  $\alpha$ -decay and spontaneous fission (Hotokezaka et al., 2016; Barnes et al., 2016).

One of the most important features of kilonovae/macronovae is a high opacity  $\kappa \approx 10 \text{ cm}^2/\text{g}$  when lanthanide elements substantially exist in the ejecta (Barnes & Kasen, 2013; Kasen et al., 2013; Tanaka & Hotokezaka, 2013; Tanaka et al., 2017). This high opacity delays the peak time and the color at the peak becomes redder (red kilonova/macronova). In the case that lanthanides are absent, the opacity is rather low  $\kappa \approx 0.1\text{--}1 \text{ cm}^2/\text{g}$  (Kasen et al., 2015; Tanaka et al., 2017) similar to that of the iron group (blue kilonova/macronova).

AT2017gfo rises to  $\approx 10^{42} \text{ erg/s}$  on a time scale of  $\approx 0.5 \text{ day}$  and the early spectrum at  $\approx 1.5 \text{ days}$  can be broadly described a thermal spectrum with  $T \approx 5000 \text{ K}$  (e.g. Pian et al. 2017; Smartt et al. 2017). This requires an ejecta component of  $\sim 0.01 M_{\odot}$  that does not contain a significant amount of lanthanides. At a few days after the merger, the bolometric light curve declines approximately as  $\approx t^{-1.3}$ , then it starts to decline steeper around 6 days (e.g. Cowperthwaite et al. 2017; Drout et al. 2017; Kasliwal et al. 2017; Waxman et al. 2017). The late spectral structure is broadly consistent with a kilonova/macronova model of which the mass fraction of lanthanides is  $\approx 10^{-3}\text{--}10^{-2}$  and for which another ejecta component with  $\sim 0.04 M_{\odot}$  is required (Kasen et al. 2017; Tanaka et al. 2017; Metzger 2017b; Waxman et al. 2017; Perego et al. 2017; Villar et al. 2017). Although specific atoms are not identified in the optical-nIR signal, the composition of the ejecta that can consistently explain the observed signal indicates the following:

- The early emission requires a component of  $\sim 0.01 M_{\odot}$  without a significant contamination of lanthanides, i.e.,  $A < 140$ .
- The late emission requires a component of  $\sim 0.04 M_{\odot}$  containing lanthanides (the mass fraction of  $\sim 10^{-3}\text{--}0.01$ ).
- The decline rate of the bolometric light curve is consistent with that expected from the heating rate resulting from an assembly of numerous  $\beta$ -decay chains.

There are uncertainties in the mass estimates by a factor of a few due to the unknown composition and profile of the ejecta. It is worth noting that the mass fraction of lanthanides out of the total  $r$ -process elements of  $\approx 10^{-3}\text{--}10^{-2}$  is smaller than the expectation from the solar matter with  $A_{\text{min}} = 90$  by a factor of  $\approx 10\text{--}100$  and it is rather consistent with the one for  $A_{\text{min}} = 69$ , of which the mass fraction is  $\sim 0.01$ . This implies that a significant amount of the first peak  $r$ -process elements may be synthesized in the ejecta. Note however that lanthanide-rich materials moving at slow velocities may not be seen in the optical-nIR data. Therefore, it is possible that the actual mass fraction of lanthanides is higher than that indicated by the observed data.

Overall there is a remarkable consistency between the rates of sGRBs and GW170817, the mass ejection observed in kilonova/macronova candidates and in AT2017gfo, and the estimates of  $R_{\text{MW}}$  and  $m_r$  from  $r$ -process elements observations. This clearly motivates us to turn to the question addressed now - whether mergers are consistent with the observed chemical history of the Milky Way. However, before turning to that we discuss the delay time of mergers and the natal kicks.

### 3 Merger time and Natal Kicks

The merger time and the natal kicks have an important effect on both the total amount of  $r$ -process nucleosynthesis and on the temporal evolution.

(i) *Merger time distribution:* The orbits of binary neutron stars decay due to gravitational-wave radiation. The time until merger,  $\tau_{\text{GW}}$ , is related to the initial semi-major axis,  $a$ , and eccentricity,  $e$ , as  $\tau_{\text{GW}} \propto a^4(1 - e^2)^{7/2}$ . The merger time is very sensitive to the initial semi-major axis, e.g., a difference in  $a$  by a factor of 4 corresponds to a different merger time by a factor of 256. Given an initial semi-major axis distribution,  $dN/da \propto a^{-\alpha}$ , the delay-time distribution is  $dN/d\tau_{\text{GW}} \propto \tau_{\text{GW}}^{-(\alpha-3)/4}$ . Therefore, in order to get a somewhat steep delay-time distribution, the initial semi-major axis distribution must be very steep.

Observationally, neutron star binaries exhibit a range of delay times between their formation and mergers. For instance, the galactic binary neutron stars have merger times distributed in different time scales from  $< 100$  Myr to longer than a Hubble time (Lorimer, 2008). Furthermore, the redshift distribution of sGRBs also shows that sGRBs occur with the delay time distribution of  $t^{-0.8^{+0.25}_{-0.24}}$  from the cosmic star formation rate (Wanderman & Piran, 2015)<sup>1</sup>. Finally, GW170817 occurred in an S0-type galaxy of which the star formation rate is very low and the time delay between the double neutron star formation and the merger is likely  $\gtrsim 1$  Gyr (Blanchard et al., 2017; Levan et al., 2017; Pan et al., 2017).

(ii) *Kick:* A crucial ingredient in the formation of binary neutron star systems is the kick imposed on the center of mass during the stellar collapse that leads to the formation of the second born neutron star. Two factors contribute to the change in the center of mass velocity. The first is simply the amount of mass ejected during the collapse,  $\Delta M$ . The second is the asymmetry in the collapse, and it is proportional to  $\vec{v}_k$ , the kick velocity imparted to the newly born neutron star by the ejected mass. The distributions of  $\Delta M$  and  $\vec{v}_k$  have been studied both directly from observations of Galactic binary neutron stars' orbital parameters (Fryer & Kalogera, 1997; Wex et al., 2000; van den Heuvel, 2004; Piran & Shaviv, 2005; Thorsett et al., 2005; Stairs et al., 2006; Kalogera et al., 2007; Ferdman et al., 2014; Dall'Osso et al., 2014; Beniamini & Piran, 2016; Tauris et al., 2017) and in combination with population synthesis models (Podsiadlowski et al., 2004; Wang et al., 2006; Willems et al., 2006; Belczynski et al., 2008; Wong et al., 2010; Schwab et al., 2010). The emerging evidence points towards a bimodal population of stellar collapses in those systems. The second collapse in the majority of systems involves small amounts of mass ejection  $\Delta M \lesssim 0.5M_{\odot}$  and weak kicks  $v_k \lesssim 30 \text{ km s}^{-1}$ . A neutron star formation scenario of this kind has been suggested based on various theoretical grounds (Miyaji et al., 1980; Nomoto, 1987; Dewi & Pols, 2003; Ivanova et al., 2003; Podsiadlowski et al., 2005; Tauris et al., 2015). Only a minority of the systems have formed via a standard supernova involving larger mass ejection of  $\sim 2.2M_{\odot}$  and kick velocities of up to  $400 \text{ km s}^{-1}$ . The observed orbital parameters of binary neutron star systems are also consistent with a possible correlation between the kick velocities and mass ejections (Beniamini & Piran, 2016). Specifically, if the shell always receives the same speed due to the explosion and has a similar degree of asymmetry, then there should be a linear correlation between the kick imparted to the neutron star and the amount of mass ejected. Note that this model is consistent with the existence of the two groups of systems described above.

The distribution of binary neutron star systems' center of mass velocities has important implications for  $r$ -process formation both in dwarf galaxies and inside our Galaxy. We consider first the former case. In recent years, Ji et al. (2016a) and Roederer et al. (2016) reported on the discovery of an  $r$ -process enriched UFD galaxy Reticulum II. The total stellar luminosity of Reticulum II is only  $\sim 10^3 L_{\odot}$  and the velocity dispersion is  $\sim 4 \text{ km/s}$  (Walker et al., 2015). Based on this detection, Bramante & Linden (2016) argued against a neutron star merger origin for this material, suggesting that the kick imparted on the system during the formation of the second born neutron star, would have ejected the binary out of such a low mass galaxy. An additional issue is that UFDs are composed of very old stellar material, implying that the binary neutron star should merge within the first  $\sim \text{Gyr}$  of its formation (before star formation ceases), in order to successfully enrich future stars with  $r$ -process material. Whether or not a significant population of such rapid mergers

<sup>1</sup>The upper and lower values show the  $1\sigma$  uncertain interval. Note that the mean and  $\sigma$  values depend on the shape of the cosmic star formation history.

exist, crucially depends on the initial distribution of binary separations. Beniamini et al. (2016a) considered the distributions of mass ejections and kicks as implied by Galactic binary neutron star observations. They have shown that a large fraction of systems would have center of mass velocities  $< 15 \text{ km s}^{-1}$  (comparable to the lowest escape velocities from UFDs). Furthermore, two of the ten binary neutron star systems (that do not reside in globular clusters and for which the orbital parameters can be estimated) have short spin-down times, implying small initial separations and short overall lifetimes. One of these is the double pulsar, which also has a small observed proper motion  $\lesssim 10 \text{ km s}^{-1}$  (Kramer et al., 2006), demonstrating that “rapid mergers” can have slow center of mass velocities. Beniamini et al. (2016a) have used these observations to show that a significant fraction ( $0.06 \lesssim f \lesssim 0.6$ ) of binary neutron star systems are expected to both remain confined in UFD galaxies and merge within less than a Gyr.

Finally, we consider the effects of natal kicks on  $r$ -process formation in our own Galaxy. The observation of  $r$ -process elements in stars with values of  $[\text{Fe}/\text{H}] \approx -3$  and below, suggests a significant amount of  $r$ -process formation in the first few Myr since the Galaxy’s formation. This again, has been used as an argument against a neutron star merger origin (Argast et al., 2004). However, the small initial separations of some binary neutron star systems inferred from observations, as well as the fact that a fraction of systems can increase their eccentricity and/or reduce their separation as a result of kicks, both contribute to a significant population of “rapid mergers” (Beniamini et al., 2016a). These may help account for the rise in  $r$ -process abundances at early times. Furthermore, even with a delay of few tens of Myrs between the SNe leading to the formation of the neutron star’s in a binary neutron star system and their eventual merger, the binary neutron star can travel a large distance from their birth place. Thus, mergers can naturally account for the observations of significant amounts of  $r$ -process material in some low metallicities halo stars in the Galaxy and to the large fluctuations in  $[\text{Eu}/\text{Fe}]$  in metal poor stars.

## 4 Galactic Eu Evolution

We already noted that the large fluctuations in  $[\text{Eu}/\text{Fe}]$  are consistent with rare events (Piran et al., 2014) and the large amounts of heavy  $r$ -process material observed in some low metallicity stars put a lower limit on the yield of each event (Macias & Ramirez-Ruiz, 2016). Depending on the origin of these low metallicity halo stars, this may require a short minimal time delay between the star formation and the first merger - an issue to which return later (Argast et al., 2004; Matteucci et al., 2014; Hirai et al., 2015; Shen et al., 2015; van de Voort et al., 2015; Ishimaru et al., 2015; Wehmeyer et al., 2015; Cescutti et al., 2015; Côté et al., 2016). Here, we focus on the late time chemical evolution of  $[\text{Eu}/\text{Fe}]$  of the Milky Way and consider that the abundances of europium and  $\alpha$ -elements trace the  $r$ -process production and cc-SNe history, respectively. The abundance distribution of iron follows a combination of cc-SNe and SNe Ia. Remarkably,  $[\text{Eu}/\text{Fe}]$  and  $[\alpha/\text{Fe}]$  evolve quite similarly (indistinguishable within uncertainties) for  $[\text{Fe}/\text{H}] \gtrsim -1$  (Fig. 7). Roughly speaking, the similarity in the mean value of  $[\alpha/\text{Fe}]$  and  $[\text{Eu}/\text{Fe}]$  means that a significant fraction of europium must be produced before the typical time it takes SNe Ia start to produce iron. This feature is naturally explained if the  $r$ -process sources immediately follow the Galactic star formation (Argast et al., 2004; Matteucci et al., 2014; Ishimaru et al., 2015; Côté et al., 2016).

It has been claimed that the observed  $[\text{Eu}/\text{Fe}]$  distribution for  $[\text{Fe}/\text{H}] \gtrsim -1$  can be reproduced by neutron star mergers with a very steep delay time distribution or a constant delay time of  $\sim 100$  Myr (Matteucci et al., 2014; Wehmeyer et al., 2015; Côté et al., 2016). Recently, Côté et al. (2016) and Komiya & Shigeyama (2016) claimed that this late-time behavior of  $[\text{Eu}/\text{Fe}]$  is inconsistent with the delay time distribution  $\propto t^{-1}$ . However, neutron star binaries exhibit a range of delay times between their formation and mergers (see §3). In the followings, we discuss whether such a delay time distribution is compatible to the galactic distribution of  $[\text{Eu}/\text{Fe}]$  for  $[\text{Fe}/\text{H}] > -1$ .

Before discussing details of the Galactic chemical evolution, let us focus on the event rate of core-collapse SNe, SNe Ia, and mergers, and the total amount of iron and  $r$ -process elements produced by these events. We define a simple form of the delay time distribution as

$$D_i(t) = \frac{C_i \theta(t - t_{\min})}{t^{b_i}}, \quad (6)$$

where  $t$  is the delay time between a SN Ia or a merger and the time when the progenitor is formed,  $t_{\min}$  is the minimal delay time,  $C_i$  is a normalization factor, which is calibrated by the local event rates. For SNe Ia, we take  $b_i = 1$  as inferred from observations (e.g. Totani et al. 2008; Maoz et al. 2014).

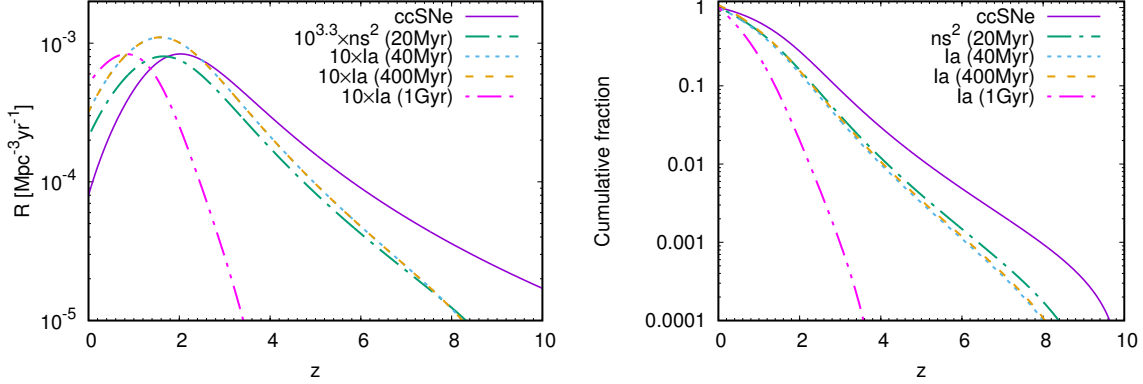


Figure 5: The volumetric event rate of cc-SNe, SNe Ia, and neutron star mergers (*left*) and the cumulative fraction (*right*). The rate of cc-SNe is assumed to follow the cosmic star formation history (Madau & Dickinson, 2014). SNe Ia and mergers are assumed to follow it with delay times distributed as  $\propto t^{-1}$ . The minimal delay time of each model is shown in parentheses.

The event rate at a given time is obtained by integrating  $D_i(t)$  with the star formation rate. Figure 5 shows the rate and cumulative fraction of cc-SNe following the cosmic star formation rate (Madau & Dickinson, 2014), type Ia SNe with minimal delay times of 40, 400,  $10^3$  Myr (Totani et al., 2008; Maoz et al., 2014), and neutron star mergers with  $b_{\text{ns}} = 1$  and a minimal delay time of 20 Myr. Given these rates and the produced mass of each element per event, we calculate, following Maoz & Graur (2017), the ratio of the total amount of elements produced by each phenomenon. Figure 6 shows  $[M_r/M_{\text{Fe}}]$  and  $[M_\alpha/M_{\text{Fe}}]$  as a function of  $[M_{\text{Fe}}/M_{\text{H}}]$ , where we assume  $\alpha$ -elements are produced by cc-SNe, iron is produced by cc-SNe and SNe Ia, and  $r$ -process elements are produced by neutron star mergers. These quantities are normalized such that  $[M_X/M_{\text{Fe}}]$  is zero at  $[M_{\text{Fe}}/M_{\text{H}}] = 0$ . The different curves correspond to the different minimal delay times of SNe Ia.

$[M_\alpha/M_{\text{Fe}}]$  decreases with  $[M_{\text{Fe}}/M_{\text{H}}]$  for  $[M_{\text{Fe}}/M_{\text{H}}] > -1$ . This is consistent with metal poor star measurements as shown in Fig. 7. However, the decline rates of  $[M_r/M_{\text{Fe}}]$  are always slower than those of  $\alpha$ -elements. The production rate of  $\alpha$ -elements drops when the star formation rate drops. On the contrary, iron and  $r$ -process elements are still produced by SNe Ia and mergers that have long delay times  $\gtrsim 1$  Gyr. This feature can be also seen in the cumulative fraction of events (the left panel of Fig. 5). In the neutron merger scenario, this slow decline of  $r$ -process elements compared to  $\alpha$ -elements is inconsistent with the abundances of stars in the solar neighborhood.

#### 4.1 A simple one zone model

We now turn to discuss the Galactic chemical evolution with a simple one zone model. The total mass of  $\alpha$ -elements in the ISM is given by

$$\frac{dM_\alpha}{dt} = m_\alpha C_{\text{cc}} \Psi(t) - M_\alpha f(t), \quad (7)$$

where  $\Psi(t)$  is the star formation rate of the Milky Way (mass per unit time),  $m_\alpha$  is the mass of  $\alpha$ -elements produced per cc-SN,  $C_{\text{cc}}$  is the cc-SN rate per unit mass, and  $f(t)$  is the mass-loss rate of the element in the ISM due to star formation and the galactic outflow. It is often assumed that the outflow rate is proportional to the star formation rate with a delay of the lifetimes of massive stars. Since we consider time scales much longer than the lifetimes of massive stars the outflow rate

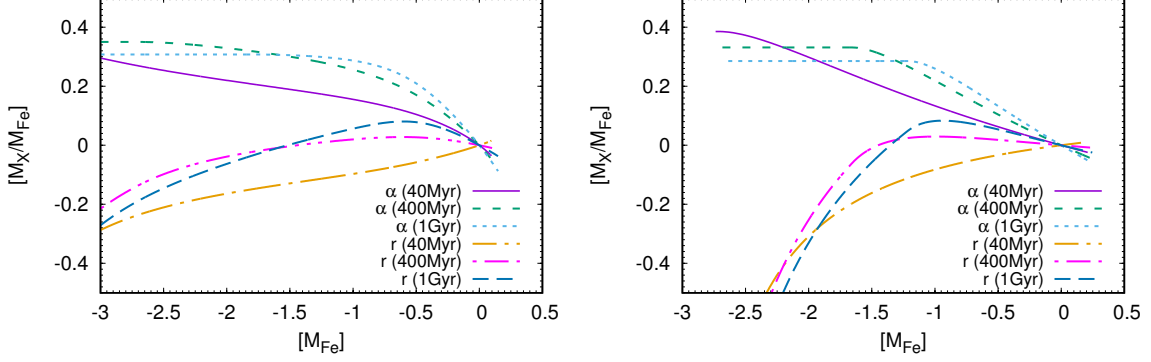


Figure 6: The logarithmic ratio of the produced mass of  $\alpha$  and  $r$ -process elements as a function of the produced iron mass. The values in parentheses show the minimal delay time of SNe Ia in each model. The star formation history is assumed to follow the cosmic star formation history (*left*) or be constant over time (*right*).

is considered to be proportional to the star formation rate:

$$f(t) = (\text{absorption rate by star formation} + \text{outflow rate})/M_{\text{ISM}} \quad (8)$$

$$= (1 + o) \frac{\Psi(t)}{M_{\text{ISM}}}, \quad (9)$$

where  $o(t)$  is the outflow rate normalized by the star formation rate, which is likely smaller than unity,  $M_{\text{ISM}}$  is the total mass of the ISM. Here, we assume  $M_{\text{ISM}} \approx 10^{10} M_{\odot}$  at  $z = 0$ . For the cosmic star formation history case, to estimate  $M_{\text{ISM}}$  as a function of time, we use the Kennicutt-Schmit relation  $\Psi \propto M_{\text{ISM}}^{1.4}$  for a given  $\Psi(t)$ . Using these relations, Eq. (7) has simple solutions in the following two limits:

$$M_{\alpha}(t) \approx \begin{cases} m_{\alpha} C_{cc} M_{*}(t) & (M_{*} \ll M_{\text{ISM}}), \\ \frac{m_{\alpha} C_{cc}}{(1+o)} M_{\text{ISM}}(t) & (M_{*} \gg M_{\text{ISM}}), \end{cases} \quad (10)$$

where  $M_{*}$  is the total stellar mass. At early times, the mass of  $\alpha$ -elements in the ISM increases linearly with the total stellar mass. Then, once the total stellar mass is larger than  $M_{\text{ISM}}$  the mass of  $\alpha$ -elements approaches to a constant value.

For neutron star mergers and for type Ia SNe, the production history involves the delay time (relative to the star formation rate) distribution. Thus, the total mass of these elements evolves differently from that of the  $\alpha$ -elements:

$$\frac{dM_{\text{Fe}}}{dt} = m_{\text{Fe, cc}} C_{cc} \Psi(t) + m_{\text{Fe, Ia}} \int_0^t dt' D_{\text{Ia}}(t-t') \Psi(t') - M_{\text{Fe}}(t) f(t), \quad (11)$$

$$\frac{dM_r}{dt} = m_r \int_0^t dt' D_{\text{ns}}(t-t') \Psi(t') - M_r(t) f(t). \quad (12)$$

At late times ( $M_{*} \gg M_{\text{ISM}}$ ), the mass of  $r$ -process elements is given by

$$M_r(t) \approx \frac{m_r}{(1+o)} \frac{\int_0^t D_{\text{ns}}(t') \cdot \Psi(t') dt'}{\Psi(t)} M_{\text{ISM}}(t). \quad (13)$$

This increases logarithmically for  $b_i = 1$  if the star formation rate is constant. When we convert europium abundances to the total  $r$ -process abundances, we use the solar  $r$ -process abundance pattern. As noted in §2.1, this procedure depends on the minimal atomic mass number of  $r$ -process elements synthesized in mergers,  $A_{\text{min}}$ . In the following, we use  $A_{\text{min}} = 69$ .

## 4.2 A Comparison with Observations

Figure 7 shows that the observed  $[\text{Mg}/\text{Fe}]$  and  $[\text{Eu}/\text{Fe}]$  for stars from SAGA database (Suda et al. 2008 and references therein). The mean value of the observed  $[\text{Mg}/\text{Fe}]$  is roughly a constant up to  $[\text{Fe}/\text{H}] \approx -1$ . Then it gradually decreases towards its value today,  $\approx 1/3$  of this constant. This is usually interpreted as due to the copious production of iron (without the production of significant amounts of  $\alpha$ -elements) by SNe Ia that begin to take place at around  $[\text{Fe}/\text{H}] \approx -1$  (e.g. Nomoto et al. 2013 and references therein, but see also Maoz & Graur 2017 for an alternative interpretation).

The resulting evolutions of  $[\text{Mg}/\text{Fe}]$  and  $[\text{Eu}/\text{Fe}]$  are shown in Fig. 7. Here, we examine two cases (i) a cosmic star formation history (left panel) and (ii) a constant star formation history (right panel). The motivation for considering these star formation rate histories is that interestingly the Galactic star formation rate history is not so clear. The cosmic star formation rate, mimics well the other possibility of an early ( $\leq 1\text{Gyr}$ ) star formation peak and one suggested approximation is a constant star formation. The input parameters of each case are listed in Table 1. Here, we fix the minimal delay time of neutron star mergers to be 20 Myr and it extends to longer delay times as  $\propto t^{-b_{\text{ns}}}$ , where  $b_{\text{ns}}$  is set to be 1 or 1.5. While 20 Myr might look short, this minimal delay time is consistent with the observed redshift distribution and peak flux of sGRBs (Wanderman & Piran, 2015). Those authors find that the distribution of time delays  $\propto t^{-0.8^{+0.25}_{-0.24}}$  for  $t > 20$  Myr is consistent with the observations. We show that the  $[\text{Mg}/\text{Fe}]$  and  $[\text{Eu}/\text{Fe}]$  evolutions with different minimal delay times of 40, 400, and 1000 Myr for SNe Ia (see, e.g., Totani et al. 2008; Maoz et al. 2014 for the SNe Ia delay time distribution).

Table 1: The input parameters for the one zone model. A value in a parenthesis is for the constant SFR case.

$m_{\text{Mg}}$	$0.12M_{\odot}/\text{event}$
$m_{\text{Fe, cc}}$	$0.074M_{\odot}/\text{event}$
$m_{\text{Fe, Ia}}$	$0.7M_{\odot}/\text{event}$
$m_r$	$0.05 (0.06)M_{\odot}/\text{event}$
$C_{\text{cc}}$	$8 \cdot 10^{-3}M_{\odot}^{-1}$
$C_{\text{Ia}}$	$1.6 \cdot 10^{-3}M_{\odot}^{-1}$
$C_{\text{ns}}$	$7 \cdot 10^{-6}M_{\odot}^{-1}$
$X_{\text{H}}$	0.75
$o$	0.25

The expected decline rate of  $[\text{Eu}/\text{Fe}]$  is shallower than  $[\text{Mg}/\text{Fe}]$  because of the delay of mergers (Fig. 7) relative to star formation.  $[\text{Eu}/\text{Fe}]$  even increases with  $[\text{Fe}/\text{H}]$  if the minimal time delay of neutron star mergers is comparable to that of SNe Ia (see also Côté et al. 2016). For the constant star formation case, the decline rates for both  $[\text{Mg}/\text{Fe}]$  and  $[\text{Eu}/\text{Fe}]$  are steeper than those for the cosmic one, but the decline of  $[\text{Eu}/\text{Fe}]$  is still slower than the observed one. The bottom panels of Fig. 7 show the evolution for a steeper delay time distribution,  $b_{\text{ns}} = 1.5$ , for neutron star mergers. As a larger population of mergers follow star formation, the decline rate of  $[\text{Eu}/\text{Fe}]$  is more similar to  $[\text{Mg}/\text{Fe}]$ , suggesting that the declining rate of  $[\text{Eu}/\text{Fe}]$  of stars in the solar neighborhood can be explained with a somewhat steep delay time distribution and with that a minimal delay time of mergers are much shorter than that of SNe Ia. However, such a steep delay time distribution is inconsistent with the distribution,  $\propto t^{-0.8 \pm 0.25}$ , derived from the redshift distribution of sGRBs (Wanderman & Piran, 2015). Furthermore, if the merger rate following star formation is much higher than that with longer time delays, it results in an overproduction of  $r$ -process elements in the Galaxy, given the produced  $r$ -process mass of  $\approx 0.05M_{\odot}$  and rate estimated from GW170817 (the time delay of GW170817 is  $\sim 1\text{--}10$  Gyr).

The neutron star merger rate used in this section corresponds to a Galactic rate of  $\approx 10\text{Myr}^{-1}$ . This is slightly smaller than the one inferred from GW170817. Note, however, that for the question of  $r$ -process nucleosynthesis the normalization of the merger rate this is degenerate with the mass produced per event as discussed in §2.1. Furthermore, because of the natal kicks involved in the

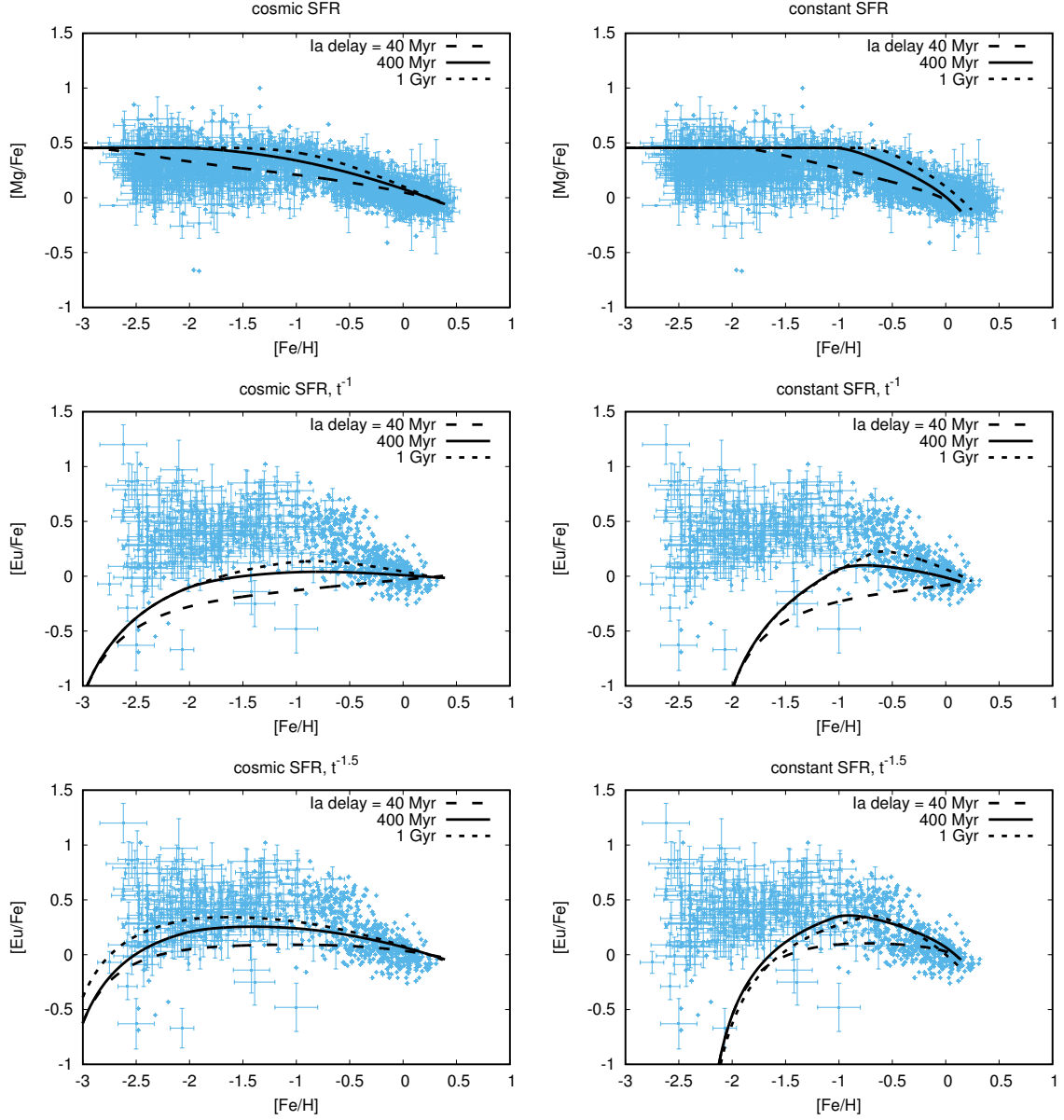


Figure 7: Magnesium (*top*) and europium (*middle* and *bottom*) abundance evolutions of the Milky Way. Here, the minimum delay time of SNe Ia is set to be 40 (dashed), 400 (solid), and 1000 Myr (short dashed curve). The minimum delay time of neutron star mergers is chosen to be 20 Myr and their delay time distribution is set to be  $\propto t^{-1}$  (*middle*) and  $\propto t^{-1.5}$  (*bottom*). The star formation history is assumed to follow the cosmic star formation history (*left*) and to be a constant with time (*right*). Also shown are the observed data of the magnesium and europium abundances of metal poor stars as blue points from SAGA database (Suda et al., 2008).

formation of neutron star binaries, a fraction of neutron star mergers occur outside the Galactic disk and they do not contribute to the Galactic chemical evolution.

## 5 Summary and Discussions

We have discussed that various measurements and theoretical estimates related to the origin of  $r$ -process elements including: the estimated rates of mergers and the estimates of yields of  $r$ -process material in each event, the total abundance of heavy  $r$ -process elements in the Milky Way, the abundance of radioactive elements in the early solar system and the current deposition rate, the abundance of heavy  $r$ -process material in dwarf galaxies, and the recent observations of the kilonova/macronova associated with GW170817. We have shown that all these are compatible with the model in which compact binary mergers are the dominant source of heavy  $r$ -process elements in the Universe.

Our main findings are: (i) The rate and mass of  $r$ -process elements produced per event inferred from the europium abundances of Galactic stars, the geological abundances of radioactive elements, and the  $r$ -process enrichment of dwarf galaxies are consistent with each other. The inferred mass per event is  $3 \cdot 10^{-2} \lesssim m_r \lesssim 3 \cdot 10^{-1} M_\odot$  for  $A_{\min} = 69$  and  $7 \cdot 10^{-3} \lesssim m_r \lesssim 7 \cdot 10^{-2} M_\odot$  for  $A_{\min} = 90$ . (ii) The rate and mass of  $r$ -process elements produced per event inferred from the optical-nIR signal (kilonova/macronova) of GW170817 are enough to explain the total amount of  $r$ -process elements in the Milky Way and consistent with the other measurements. The rate and mass are also consistent with the rate of sGRBs and the ejecta mass estimates of the kilonova/macronova candidates associated with nearby sGRBs. (iii) The natal kicks of binary neutron stars and the time delay between the formation and merger may reduce a population of mergers that contribute to the  $r$ -process enrichment, in particular, for small dwarf galaxies, of which the escape velocity is low and the star formation lasts for a relatively short time scale.

On the other hand, when we studied the Galactic chemical evolution, we encountered some problems with the simple one zone model. We compared the Galactic chemical evolution of iron,  $\alpha$ -elements, and  $r$ -process elements (specifically europium) with a model in which mergers follow the star formation rate with a delay time distribution,  $\alpha$ -elements are produced by cc-SNe and iron is produced predominantly by type Ia SNe but also by cc-SNe. The difficulty stems from the fact that the distribution of  $[\text{Eu}/\text{Fe}]$  for  $[\text{Fe}/\text{H}] \gtrsim -1$  is quite similar to that of  $[\alpha/\text{Fe}]$ . Both fall by about a factor of 3 between  $[\text{Fe}/\text{H}] \approx -1$  and the solar value. This indicates that a significant fraction of both  $\alpha$ -elements and  $r$ -process elements is produced before SNe Ia begin to produce significant amounts of iron. The first is natural as we expect that  $\alpha$ -elements are produced by cc-SNe. However, this is somewhat problematic for the neutron star merger scenario as  $r$ -process events are expected to be delayed relative to the cc-SNe. The expected theoretical distribution is  $\propto t^{-1}$  (recall that this is also roughly the distribution implied by sGRBs). In fact an intrinsic problem arises here since we have assumed that at late times both type Ia SNe and compact binary mergers follow the star formation rate convoluted with a  $t^{-1}$  time delay distribution. This makes the late time decrease in  $[\text{Eu}/\text{Fe}]$  problematic. Unlike earlier works that suggest problems with early formation of  $r$ -process elements within the merger model we stress here a problem at late times (higher metallicity problem).

The model can fit the data if we stretch the parameters. Extending the time delay for the onset of type Ia SNe to 1Gyr, setting the minimal time delay of mergers at 20 Myr and employing a time delay distribution  $\propto t^{-1.5}$ . In this case a significant fraction of mergers are pushed back to early times and the resulting  $[\text{Eu}/\text{Fe}]$  is consistent with observations. As mentioned earlier such a distribution is inconsistent with theoretical expectations and with sGRB observations, which show  $t^{-0.80 \pm .25}$  (Wanderman & Piran, 2015). Furthermore, such a steep distribution combined with the rate, mass estimate, and time delay of GW180817 seems to result in an overproduction of  $r$ -process elements in the Milky Way.

This tension between the chemical evolution observations and our model is disturbing. However, before turning to conclude that mergers are inconsistent as sources of heavy  $r$ -process elements we should consider both the simplicity of our model and the complexity of the observed data.

Concerning the observations we note that there are several different samples of abundance measurements and it is not clear how to combine them. Furthermore, the abundances are compared to

[Fe/H]. Especially at low metallicities [Fe/H] may not vary at the same rate with time in different regions of the Galaxy. This latter fact is particularly important if the star formation history varies strongly in different regimes of the Galaxy. In fact, a larger sample of red giants in the APOGEE survey shows an  $\alpha$ -abundance distribution different from that seen in the solar neighborhood ( $[\alpha/\text{Fe}]$  is lower for red giants at lower Galactic scale heights; Hayden et al. 2015). However, the  $r$ -process abundance distribution of those stars has not yet been determined.

As for the theoretical model, we have made some strong simplifying assumptions. First we have used one zone model with a single star formation history. It is clear that different regimes at the Galaxy (i.e. the bulge and the disk) formed at different times. Similarly we ignored the effect of merging dwarf galaxies and the effect that mergers can occur in low metallicity regions due to natal kicks that launch neutron star binaries from one region in the Galaxy to another. Depending on their star formation histories such events could have either enriched the Galaxy with  $r$ -process rich material or with very low metallicity material (Hirai et al., 2015; Shen et al., 2015; van de Voort et al., 2015; Ishimaru et al., 2015; Naiman et al., 2017; Hirai et al., 2017). The overall sign of this effect is not clear. Finally we have assumed that the type Ia rate is also dictated by gravitational radiation decay with a given minimal time delay followed by  $t^{-1}$  distribution. While this is supported by observations (Totani et al., 2008; Maoz et al., 2014). Changing this time delay distribution to one dominated, for example, by the formation rate of white dwarfs (e.g. Yungelson & Livio 2000 but see also Hachisu et al. 2008) would change the [Fe/H] and yield a different chemical evolutions that may resolve some of the problems found here.

More neutron star mergers will be discovered in the upcoming observation runs of Advanced LIGO/Virgo. KAGRA and LIGO-India will also join in near future and adding these two detectors will improve the localization and the duty cycle. Identifying the host galaxies of mergers will reveal the event rate and delay time distribution of mergers. Furthermore, kilonovae/macronovae of different events may have different features, e.g., the ejecta mass and the fraction of lanthanides. In addition to binary neutron star mergers, GW signals from black hole-neutron star mergers are expected to be discovered. This will reveal the role of black hole-neutron star mergers for  $r$ -process material production in the Universe. Therefore, future GW and EM observations will give us better understanding on the  $r$ -process budget and on the variation in the abundance patterns of  $r$ -rich extremely metal poor stars.

We thank Chia-Yu Hu, Dan Maoz, Brian Metzger, Ehud Nakar, Yong-Zhong Qian, Masaru Shibata, Masaomi Tanaka, and Shinya Wanajo for useful discussions. K.H. was supported by the Flatiron Fellowship at the Simons Foundation and the Lyman Spitzer Jr. Fellowship awarded by Department of Astrophysical Sciences at Princeton University. T.P. was partially supported by an advanced ERC grant TReX and by a grant from the Templeton foundation. We acknowledge kind hospitality at the Flatiron institute while some of this research was done.

## References

- Abadie, J., Abbott, B. P., Abbott, R., et al. 2010, *Classical and Quantum Gravity*, 27, 173001
- Abbott, B. P., et al. 2017a, *Astrophys. J.*, 848, L13
- . 2017b, *Phys. Rev. Lett.*, 119, 161101
- Abbott, B. P., Abbott, R., Abbott, T. D., et al. 2017, *ApJL*, 848, L12
- Abbott, B. P., et al. 2017, Submitted to: *Astrophys. J.*, arXiv:1710.05838
- Alexander, K. D., et al. 2017, *Astrophys. J.*, 848, L21
- Andreoni, I., et al. 2017, Submitted to: *Publ. Astron. Soc. Austral.*, arXiv:1710.05846
- Arcavi, I., Hosseinzadeh, G., Howell, D. A., et al. 2017, *Nature*, 551, 64
- Arcones, A., & Martínez-Pinedo, G. 2011, *PRC*, 83, 045809
- Arcones, A., & Thielemann, F.-K. 2013, *Journal of Physics G Nuclear Physics*, 40, 013201

Argast, D., Samland, M., Thielemann, F.-K., & Qian, Y.-Z. 2004, *A&A*, 416, 997

Arnould, M., Goriely, S., & Takahashi, K. 2007, *Phys. Rep.*, 450, 97

Barnes, J., & Kasen, D. 2013, *ApJ*, 775, 18

Barnes, J., Kasen, D., Wu, M.-R., & Martínez-Pinedo, G. 2016, *ApJ*, 829, 110

Battistini, C., & Bensby, T. 2016, *A&A*, 586, A49

Bauswein, A., Ardevol Pulpillo, R., Janka, H.-T., & Goriely, S. 2014, *ApJL*, 795, L9

Bauswein, A., Goriely, S., & Janka, H.-T. 2013, *ApJ*, 773, 78

Belczynski, K., Kalogera, V., Rasio, F. A., et al. 2008, *ApJ Supplements*, 174, 223

Beniamini, P., Dvorkin, I., & Silk, J. 2017, *ArXiv e-prints*, arXiv:1711.02683

Beniamini, P., Hotokezaka, K., & Piran, T. 2016a, *ApJL*, 829, L13

—. 2016b, *ApJ*, 832, 149

Beniamini, P., & Piran, T. 2016, *MNRAS*, 456, 4089

Berger, E. 2014, *ARA&A*, 52, 43

Berger, E., Fong, W., & Chornock, R. 2013, *ApJL*, 774, L23

Blanchard, P. K., et al. 2017, *Astrophys. J.*, 848, L22

Bovard, L., Martin, D., Guercilena, F., et al. 2017, *ArXiv e-prints*, arXiv:1709.09630

Bramante, J., & Linden, T. 2016, *ApJ*, 826, 57

Brennecka, G. A., Weyer, S., Wadhwa, M., et al. 2010, *Science*, 327, 449

Bromberg, O., Nakar, E., Piran, T., & Sari, R. 2011, *ApJ*, 740, 100

Bromberg, O., Tchekhovskoy, A., Gottlieb, O., et al., 2017, *Arxiv*, arXiv:1710.05897

Buckley, D. A. H., et al. 2017, arXiv:1710.05855

Burbidge, G., Burbidge, R., Fowler, W., & Hoyle, F. 1957, *Rev. Mod. Phys.*, 29, 547

Caballero, O. L., McLaughlin, G. C., & Surman, R. 2012, *ApJ*, 745, 170

Cameron, A. G. W. 1957, *Chalk River Rept.*, CRL-41

Cescutti, G., Romano, D., Matteucci, F., Chiappini, C., & Hirschi, R. 2015, *A&A*, 577, A139

Chornock, R., Berger, E., Kasen, D., et al. 2017, *ApJL*, 848, L19

Ciolfi, R., Kastaun, W., Giacomazzo, B., et al. 2017, *Phys. Rev. D.*, 95, 063016

Côté, B., West, C., Heger, A., et al. 2016, *MNRAS*, 463, 3755

Côté, B., Fryer, C. L., Belczynski, K., et al. 2017, *ArXiv e-prints*, arXiv:1710.05875

Coulter, D. A., et al. 2017, arXiv:1710.05452

Cowan, J. J., Thielemann, F.-K., & Truran, J. W. 1991, *Phys. Rep.*, 208, 267

Cowperthwaite, P. S., et al. 2017, *Astrophys. J.*, 848, L17

Dall’Osso, S., Piran, T., & Shaviv, N. 2014, *MNRAS*, 438, 1005

Dessart, L., Ott, C. D., Burrows, A., Rosswog, S., & Livne, E. 2009, *ApJ*, 690, 1681

Dewi, J. D. M., & Pols, O. R. 2003, MNRAS, 344, 629

Dietrich, T., Ujevic, M., Tichy, W., Bernuzzi, S., & Brüggemann, B. 2017, Phys. Rev. D. , 95, 024029

Drout, M. R., et al. 2017, arXiv:1710.05443

East, W. E., & Pretorius, F. 2012, ApJL, 760, L4

Eichler, D., Livio, M., Piran, T., & Schramm, D. N. 1989, Nature, 340, 126

Eichler, M., Arcones, A., Kelic, A., et al. 2015, ApJ, 808, 30

Ellis, J., Fields, B. D., & Schramm, D. N. 1996, ApJ, 470, 1227

Evans, P. A., et al. 2017, arXiv:1710.05437

Farouqi, K., Kratz, K.-L., Pfeiffer, B., et al. 2010, ApJ, 712, 1359

Ferdman, R. D., Stairs, I. H., Kramer, M., et al. 2014, MNRAS, 443, 2183

Fernández, R., & Metzger, B. D. 2013, MNRAS, 435, 502

Fernández, R., Quataert, E., Schwab, J., Kasen, D., & Rosswog, S. 2015, MNRAS, 449, 390

Fitoussi, C., Raisbeck, G. M., Knie, K., et al. 2008, Physical Review Letters, 101, 121101

Fong, W., Metzger, B. D., Berger, E., & Özel, F. 2016, ApJ, 831, 141

Fong, W., Berger, E., Metzger, B. D., et al. 2014, ApJ, 780, 118

Foucart, F., Deaton, M. B., Duez, M. D., et al. 2014, Phys. Rev. D. , 90, 024026

Foucart, F., Desai, D., Brege, W., et al. 2017, Classical and Quantum Gravity, 34, 044002

Fox, D. B., Frail, D. A., Price, P. A., et al. 2005, Nature, 437, 845

Frebel, A., Kirby, E. N., & Simon, J. D. 2010a, Nature, 464, 72

Frebel, A., Simon, J. D., Geha, M., & Willman, B. 2010b, ApJ, 708, 560

Frebel, A., Simon, J. D., & Kirby, E. N. 2014, ApJ, 786, 74

Freiburghaus, C., Rembges, J.-F., Rauscher, T., et al. 1999a, ApJ, 516, 381

Freiburghaus, C., Rosswog, S., & Thielemann, F.-K. 1999b, ApJL, 525, L121

Fry, B. J., Fields, B. D., & Ellis, J. R. 2016, ApJ, 827, 48

Fryer, C., & Kalogera, V. 1997, ApJ, 489, 244

Fryer, C. L., Herwig, F., Hungerford, A., & Timmes, F. X. 2006, ApJL, 646, L131

Fujibayashi, S., Kiuchi, K., Nishimura, N., Sekiguchi, Y., & Shibata, M. 2017, ArXiv e-prints, arXiv:1711.02093

Fujibayashi, S., Yoshida, T., & Sekiguchi, Y. 2015, ApJ, 810, 115

Gal-Yam, A., Fox, D. B., Price, P. A., et al. 2006, Nature, 444, 1053

Ghirlanda, G., Salafia, O. S., Pescalli, A., et al. 2016, A&A, 594, A84

Goldstein, A., Veres, P., Burns, E., et al. 2017, ApJL, 848, L14

Goriely, S. 1999, A&A, 342, 881

Goriely, S., Bauswein, A., & Janka, H.-T. 2011, ApJL, 738, L32

Goriely, S., & Janka, H.-T. 2016, MNRAS, 459, 4174

Gottlieb, O., Nakar, E., Piran, T., & Hotokezaka, K. 2017, arXiv:1710.05896

Greif, T. H., Glover, S. C. O., Bromm, V., & Klessen, R. S. 2010, ApJ, 716, 510

Grossman, D., Korobkin, O., Rosswog, S., & Piran, T. 2014, MNRAS, 439, 757

Guetta, D., & Piran, T. 2006, A&A, 453, 823

Guetta, D., & Stella, L. 2009, A&A, 498, 329

Hachisu, I., Kato, M., & Nomoto, K. 2008, ApJL, 683, L127

Haggard, D., Nynka, M., Ruan, J. J., et al. 2017, Astrophys. J., 848, L25

Hallinan, G., et al. 2017, arXiv:1710.05435

Hansen, T. T., Simon, J. D., Marshall, J. L., et al. 2017, ApJ, 838, 44

Hayden, M. R., Bovy, J., Holtzman, J. A., et al. 2015, ApJ, 808, 132

Hill, V., Plez, B., Cayrel, R., et al. 2002, A&A, 387, 560

Hirai, Y., Ishimaru, Y., Saitoh, T. R., et al. 2015, ApJ, 814, 41

Hirai, Y., Ishimaru, Y., Saitoh, T. R., et al. 2017, MNRAS, 466, 2464

Hjorth, J., Levan, A. J., Tanvir, N. R., et al. 2017, Astrophys. J., 848, L31

Hoffman, R. D., Woosley, S. E., & Qian, Y.-Z. 1997, ApJ, 482, 951

Honda, S., Aoki, W., Ishimaru, Y., Wanajo, S., & Ryan, S. G. 2006, ApJ, 643, 1180

Horesh, A., Hotokezaka, K., Piran, T., Nakar, E., & Hancock, P. 2016, ApJL, 819, L22

Hotokezaka, K., Kiuchi, K., Kyutoku, K., et al. 2013a, Phys. Rev. D, 87, 024001

Hotokezaka, K., Kyutoku, K., Tanaka, M., et al. 2013b, ApJL, 778, L16

Hotokezaka, K., Piran, T., & Paul, M. 2015, Nature Physics, 11, 1042

Hotokezaka, K., Sari, R., & Piran, T. 2017, MNRAS, 468, 91

Hotokezaka, K., Wanajo, S., Tanaka, M., et al. 2016, MNRAS, 459, 35

Ishimaru, Y., Wanajo, S., & Prantzos, N. 2015, ApJL, 804, L35

Ivanova, N., Belczynski, K., Kalogera, V., Rasio, F. A., & Taam, R. E. 2003, ApJ, 592, 475

Ji, A. P., Frebel, A., Chiti, A., & Simon, J. D. 2016a, Nature, 531, 610

Ji, A. P., Frebel, A., Simon, J. D., & Chiti, A. 2016b, ApJ, 830, 93

Jin, Z.-P., Li, X., Cano, Z., et al. 2015, ApJL, 811, L22

Jin, Z.-P., Hotokezaka, K., Li, X., et al. 2016, Nature Communications, 7, 12898

Just, O., Bauswein, A., Pulpillo, R. A., Goriely, S., & Janka, H.-T. 2015, MNRAS, 448, 541

Kalogera, V., Belczynski, K., Kim, C., O’Shaughnessy, R., & Willems, B. 2007, Phys. Rep., 442, 75

Kasen, D., Badnell, N. R., & Barnes, J. 2013, ApJ, 774, 25

Kasen, D., Fernández, R., & Metzger, B. D. 2015, MNRAS, 450, 1777

Kasen, D., Metzger, B., Barnes, J., Quataert, E., & Ramirez-Ruiz, E. 2017, Nature, 551, 80

Kasliwal, M. M., Korobkin, O., Lau, R. M., Wollaeger, R., & Fryer, C. L. 2017, ApJL, 843, L34

Kasliwal, M. M., et al. 2017, arXiv:1710.05436

Kawaguchi, K., Kyutoku, K., Nakano, H., et al. 2015, Phys. Rev. D. , 92, 024014

Kawaguchi, K., Kyutoku, K., Shibata, M., & Tanaka, M. 2016, ApJ, 825, 52

Kilpatrick, C. D., et al. 2017, arXiv:1710.05434

Kim, C., Perera, B. B. P., & McLaughlin, M. A. 2015, MNRAS, 448, 928

Kim, S., Schulze, S., Resmi, L., et al. 2017, ApJL, 850, L21

Kiuchi, K., Sekiguchi, Y., Kyutoku, K., et al. 2015, Phys. Rev. D. , 92, 064034

Komiya, Y., & Shigeyama, T. 2016, ApJ, 830, 76

Korobkin, O., Rosswog, S., Arcones, A., & Winteler, C. 2012, MNRAS, 426, 1940

Kramer, M., Stairs, I. H., Manchester, R. N., et al. 2006, Science, 314, 97

Kulkarni, S. R. 2005, ArXiv Astrophysics e-prints, arXiv:astro-ph/0510256

Kyutoku, K., Ioka, K., Okawa, H., Shibata, M., & Taniguchi, K. 2015, Phys. Rev. D. , 92, 044028

Kyutoku, K., Kiuchi, K., Sekiguchi, Y., Shibata, M., & Taniguchi, K. 2017, ArXiv e-prints, arXiv:1710.00827

Lattimer, J. M., & Schramm, D. N. 1974, ApJ, (Letters), 192, L145

Lattimer, J. M., & Schramm, D. N. 1976, ApJ, 210, 549

Lee, W. H., Ramirez-Ruiz, E., & López-Cámara, D. 2009, ApJL, 699, L93

Letarte, B., Hill, V., Tolstoy, E., et al. 2010, A&A, 523, A17

Levan, A. J., Lyman, J. D., Tanvir, N. R., et al. 2017, ApJL, 848, L28

Li, L., & Paczyński, B. 1998, ApJL, 507, L59

Li, W., Chornock, R., Leaman, J., et al. 2011, MNRAS, 412, 1473

Lippuner, J., Fernández, R., Roberts, L. F., et al. 2017, MNRAS, 472, 904

Lippuner, J., & Roberts, L. F. 2015, ApJ, 815, 82

Lipunov, V. M., Gorbovskoy, E., Kornilov, V. G., et al. 2017, ApJL, 850, L1

Lodders, K. 2003, ApJ, 591, 1220

Lorimer, D. R. 2008, Living Reviews in Relativity, 11, arXiv:0811.0762

Macias, P., & Ramirez-Ruiz, E. 2016, ArXiv e-prints, arXiv:1609.04826

Madau, P., & Dickinson, M. 2014, ARA&A, 52, 415

Malkus, A., Kneller, J. P., McLaughlin, G. C., & Surman, R. 2012, Phys. Rev. D, 86, 085015

Maoz, D., & Graur, O. 2017, ApJ, 848, 25

Maoz, D., Mannucci, F., & Nelemans, G. 2014, ARA&A, 52, 107

Margutti, R., Berger, E., Fong, W., et al. 2017, ApJL, 848, L20

Matteucci, F., Romano, D., Arcones, A., Korobkin, O., & Rosswog, S. 2014, MNRAS, 438, 2177

McCully, C., et al. 2017, Astrophys. J., 848, L32

McMillan, P. J. 2011, MNRAS, 414, 2446

Melandri, A., Baumgartner, W. H., Burrows, D. N., et al. 2013, GRB Coordinates Network, 14735, 1

Metzger, B. D. 2017, *Living Reviews in Relativity*, 20, 3

Metzger, B. D., Arcones, A., Quataert, E., & Martinez-Pinedo, G. 2010a, *MNRAS*, 402, 2771

Metzger, B. D., & Bower, G. C. 2013, *MNRAS*, arXiv:1310.4506

Metzger, B. D., & Fernández, R. 2014, *MNRAS*, 441, 3444

Metzger, B. D., Piro, A. L., & Quataert, E. 2008, *MNRAS*, 390, 781

Metzger, B. D., Martinez-Pinedo, G., Darbha, S., et al. 2010b, *MNRAS*, 406, 2650

Metzger, B. D. 2017, Arxiv, e-print, arXiv:1710.05931

Miyaji, S., Nomoto, K., Yokoi, K., & Sugimoto, D. 1980, *PASJ*, 32, 303

Moharana, R., & Piran, T. 2017, *MNRAS*, 472, L55

Mooley, K. P., Nakar, E., Hotokezaka, K., et al. 2017, ArXiv e-prints, arXiv:1711.11573

Mösta, P., Roberts, L. F., Halevi, G., et al. 2017, Arxiv, e-print, arXiv:1712.09370

Naiman, J. P., Pillepich, A., Springel, V., et al. 2017, ArXiv e-prints, arXiv:1707.03401

Nakar, E. 2007, *Phys. Rep.*, 442, 166

Nakar, E., Gal-Yam, A., & Fox, D. B. 2006, *ApJ*, 650, 281

Nakar, E., & Piran, T. 2011, *Nature*, 478, 82

Narayan, R., Piran, T., & Shemi, A. 1991, *ApJL*, 379, L17

Nicholl, M., et al. 2017, *Astrophys. J.*, 848, L18

Nishimura, N., Takiwaki, T., & Thielemann, F.-K. 2015, *ApJ*, 810, 109

Nomoto, K. 1987, *ApJ*, 322, 206

Nomoto, K., Kobayashi, C., & Tominaga, N. 2013, *ARA&A*, 51, 457

Oechslin, R., Janka, H., & Marek, A. 2007, *A & A*, 467, 395

Özel, F., Psaltis, D., Narayan, R., & Santos Villarreal, A. 2012, *ApJ*, 757, 55

Pan, Y. C., et al. 2017, arXiv:1710.05439

Paul, M., Valenta, A., Ahmad, I., et al. 2001, *ApJL*, 558, L133

Perego, A., Rosswog, S., Cabezón, R. M., et al. 2014, *MNRAS*, 443, 3134

Perego, A., Radice, D., & Bernuzzi, S. 2017, *ApJL*, 850, L37

Perley, D. A., Metzger, B. D., Granot, J., et al. 2009, *ApJ*, 696, 1871

Phinney, E. S. 1991, *ApJL*, 380, L17

Pian, E., D’Avanzo, P., Benetti, S., et al. 2017, *Nature*, 551, 67

Piran, T., Korobkin, O., & Rosswog, S. 2014, ArXiv e-prints, arXiv:1401.2166

Piran, T., Nakar, E., & Rosswog, S. 2013, *MNRAS*, 430, 2121

Piran, T., & Shaviv, N. J. 2005, *Physical Review Letters*, 94, 051102

Podsiadlowski, P., Dewi, J. D. M., Lesaffre, P., et al. 2005, *MNRAS*, 361, 1243

Podsiadlowski, P., Langer, N., Poelarends, A. J. T., et al. 2004, *ApJ*, 612, 1044

Qian, Y.-Z. 2000, *ApJL*, 534, L67

Qian, Y.-Z., & Wasserburg, G. J. 2007, *Phys. Rep.*, 442, 237

Qian, Y.-Z., & Woosley, S. E. 1996, *ApJ*, 471, 331

Radice, D., Galeazzi, F., Lippuner, J., et al. 2016, *MNRAS*, 460, 3255

Rezzolla, L., Giacomazzo, B., Baiotti, L., et al. 2011, *ApJL*, 732, L6

Roberts, L. F., Kasen, D., Lee, W. H., & Ramirez-Ruiz, E. 2011, *ApJL*, 736, L21+

Roberts, L. F., Woosley, S. E., & Hoffman, R. D. 2010, *ApJ*, 722, 954

Roederer, I. U., & Kirby, E. N. 2014, *MNRAS*, 440, 2665

Roederer, I. U., Kratz, K.-L., Frebel, A., et al. 2009, *ApJ*, 698, 1963

Roederer, I. U., Mateo, M., Bailey, III, J. I., et al. 2016, *AJ*, 151, 82

Rosswog, S. 2005, *ApJ*, 634, 1202

—. 2013, *Philosophical Transactions A*, arXiv:1210.6549, arXiv:1210.6549

Rosswog, S., Davies, M. B., Thielemann, F.-K., & Piran, T. 2000, *A&A*, 360, 171

Rosswog, S., Feindt, U., Korobkin, O., et al. 2017a, *Classical and Quantum Gravity*, 34, 104001

Rosswog, S., Liebendörfer, M., Thielemann, F.-K., et al. 1999, *A & A*, 341, 499

Rosswog, S., Piran, T., & Nakar, E. 2013, *MNRAS*, 430, 2585

Rosswog, S., Sollerman, J., Feindt, U., et al. 2017b, *ArXiv e-prints*, arXiv:1710.05445

Ruan, J. J., Nynka, M., Haggard, D., Kalogera, V., & Evans, P. 2017, *ArXiv e-prints*, arXiv:1712.02809

Ruffert, M., & Janka, H.-T. 2001, *A&A*, 380, 544

Ruiz, M., Lang, R. N., Paschalidis, V., & Shapiro, S. L. 2016, *ApJL*, 824, L6

Safarzadeh, M., & Scannapieco, E. 2017, *MNRAS*, 471, 2088

Savchenko, V., et al. 2017, *Astrophys. J.*, 848, L15

Schulreich, M. M., Breitschwerdt, D., Feige, J., & Dettbarn, C. 2017, *A&A*, 604, A81

Schwab, J., Podsiadlowski, P., & Rappaport, S. 2010, *ApJ*, 719, 722

Sekiguchi, Y., Kiuchi, K., Kyutoku, K., & Shibata, M. 2015, *Phys. Rev. D.*, 91, 064059

Shappee, B. J., et al. 2017, arXiv:1710.05432

Shen, S., Cooke, R. J., Ramirez-Ruiz, E., et al. 2015, *ApJ*, 807, 115

Shetrone, M., Venn, K. A., Tolstoy, E., et al. 2003, *AJ*, 125, 684

Shetrone, M. D., Côté, P., & Sargent, W. L. W. 2001, *ApJ*, 548, 592

Shibata, M., Fujibayashi, S., Hotokezaka, K., et al. 2017, *ArXiv e-prints*, arXiv:1710.07579

Shibata, M., & Uryū, K. ō. 2000, *Phys. Rev. D.*, 61, 064001

Siegel, D. M., & Metzger, B. D. 2017, *ArXiv e-prints*, arXiv:1705.05473

Smartt, S. J., et al. 2017, *Nature*, arXiv:1710.05841

- Snedden, C., Cowan, J. J., & Gallino, R. 2008, *ARA&A*, 46, 241
- Soares-Santos, M., et al. 2017, *Astrophys. J.*, 848, L16
- Stairs, I. H., Thorsett, S. E., Dewey, R. J., Kramer, M., & McPhee, C. A. 2006, *MNRAS*, 373, L50
- Suda, T., Katsuta, Y., Yamada, S., et al. 2008, *PASJ*, 60, 1159
- Surman, R., Caballero, O. L., McLaughlin, G. C., Just, O., & Janka, H.-T. 2013, *ArXiv e-prints*, arXiv:1312.1199
- Surman, R., McLaughlin, G. C., Ruffert, M., Janka, H., & Hix, W. R. 2008, *ApJL*, 679, L117
- Suzuki, T. K., & Nagataki, S. 2005, *ApJ*, 628, 914
- Symbalisty, E., & Schramm, D. N. 1982, *Astrophys. Lett.*, 22, 143
- Takahashi, K., Wittl, J., & Janka, H.-T. 1994, *A&A*, 286, 857
- Tanaka, M. 2016, *Advances in Astronomy*, 2016, 634197
- Tanaka, M., & Hotokezaka, K. 2013, *ApJ*, 775, 113
- Tanaka, M., et al. 2017, *Publ. Astron. Soc. Jap.*, arXiv:1710.05850
- Tanaka, M., Kato, D., Gaigalas, G., et al. 2017, *ArXiv e-prints*, arXiv:1708.09101
- Tanvir, N. R., Levan, A. J., Fruchter, A. S., et al. 2013, *Nature*, 500, 547
- Tanvir, N. R., et al. 2017, *Astrophys. J.*, 848, L27
- Tauris, T. M., Langer, N., & Podsiadlowski, P. 2015, *MNRAS*, 451, 2123
- Tauris, T. M., Kramer, M., Freire, P. C. C., et al. 2017, *ApJ*, 846, 170
- Thielemann, K. F., Eichler, M., Panov, I. V., & Wehmeyer, B. 2017, *Annual Review of Nuclear and Particle Science*, 67, annurev
- Thompson, T. A., Burrows, A., & Meyer, B. S. 2001, *ApJ*, 562, 887
- Thorsett, S. E., Dewey, R. J., & Stairs, I. H. 2005, *ApJ*, 619, 1036
- Tissot, F. L. H., Dauphas, N., & Grossman, L. 2016, *Science Advances*, 2, e1501400
- Totani, T., Morokuma, T., Oda, T., Doi, M., & Yasuda, N. 2008, *PASJ*, 60, 1327
- Troja, E., et al. 2017, *Nature*, arXiv:1710.05433
- Tsujimoto, T., Ishigaki, M. N., Shigeyama, T., & Aoki, W. 2015, *PASJ*, 67, L3
- Tsujimoto, T., & Shigeyama, T. 2014, *A&A*, 565, L5
- Tsujimoto, T., Yokoyama, T., & Bekki, K. 2017, *ApJL*, 835, L3
- Turner, G., Busfield, A., Crowther, S. A., et al. 2007, *Earth and Planetary Science Letters*, 261, 491
- Turner, G., Harrison, T. M., Holland, G., Mojzsis, S. J., & Gilmour, J. 2004, *Science*, 306, 89
- Utsumi, Y., et al. 2017, *Publ. Astron. Soc. Japan*, arXiv:1710.05848
- Valenti, S., Sand, D. J., Yang, S., et al. 2017, *Astrophys. J.*, 848, L24
- van de Voort, F., Quataert, E., Hopkins, P. F., Kereš, D., & Faucher-Giguère, C.-A. 2015, *MNRAS*, 447, 140

van den Heuvel, E. P. J. 2004, in ESA Special Publication, Vol. 552, 5th INTEGRAL Workshop on the INTEGRAL Universe, ed. V. Schoenfelder, G. Lichti, & C. Winkler, 185

Venn, K. A., Irwin, M., Shetrone, M. D., et al. 2004, *AJ*, 128, 1177

Villar, V. A., Guillochon, J., Berger, E., et al. 2017, *ApJL*, 851, L21

Vlasov, A. D., Metzger, B. D., Lippuner, J., Roberts, L. F., & Thompson, T. A. 2017, *MNRAS*, 468, 1522

Vlasov, A. D., Metzger, B. D., & Thompson, T. A. 2014, *MNRAS*, 444, 3537

Walker, M. G., Mateo, M., Olszewski, E. W., et al. 2015, *ApJ*, 808, 108

Wallner, A., Faestermann, T., Feige, J., et al. 2015, *Nature Communications*, 6, 5956

Wallner, A., Feige, J., Kinoshita, N., et al. 2016, *Nature*, 532, 69

Wanajo, S. 2013, *ApJL*, 770, L22

Wanajo, S., & Janka, H.-T. 2012, *ApJ*, 746, 180

Wanajo, S., Janka, H.-T., & Müller, B. 2011, *ApJL*, 726, L15

Wanajo, S., Sekiguchi, Y., Nishimura, N., et al. 2014, *ApJL*, 789, L39

Wanderman, D., & Piran, T. 2015, *MNRAS*, 448, 3026

Wang, C., Lai, D., & Han, J. L. 2006, *ApJ*, 639, 1007

Wasserburg, G. J., Busso, M., & Gallino, R. 1996, *ApJL*, 466, L109

Watson, D., Hjorth, J., Jakobsson, P., et al. 2006, *A&A*, 454, L123

Waxman, E., Ofek, E., Kushnir, D., & Gal-Yam, A. 2017, *ArXiv e-prints*, arXiv:1711.09638

Wehmeyer, B., Pignatari, M., & Thielemann, F.-K. 2015, *MNRAS*, 452, 1970

Wex, N., Kalogera, V., & Kramer, M. 2000, *ApJ*, 528, 401

Willems, B., Kaplan, J., Fragos, T., Kalogera, V., & Belczynski, K. 2006, *Phys. Rev. D*, 74, 043003

Winteler, C., Käppeli, R., Perego, A., et al. 2012, *ApJL*, 750, L22

Wollaeger, R. T., Korobkin, O., Fontes, C. J., et al. 2017, *ArXiv e-prints*, arXiv:1705.07084

Wong, T.-W., Willems, B., & Kalogera, V. 2010, *ApJ*, 721, 1689

Woosley, S. E., Wilson, J. R., Mathews, G. J., Hoffman, R. D., & Meyer, B. S. 1994, *ApJ*, 433, 229

Wu, M.-R., Fernández, R., Martínez-Pinedo, G., & Metzger, B. D. 2016, *MNRAS*, 463, 2323

Yang, B., Jin, Z.-P., Li, X., et al. 2015, *Nature Communications*, 6, 7323

Yungelson, L. R., & Livio, M. 2000, *ApJ*, 528, 108